

**Effects of Iron and Oxidative Stress on Cx43 Expression  
and Phosphorylation in Human Enterocytes**

by

**Ryan Szajkowski**

A Thesis submitted to the Faculty of Graduate Studies of  
The University of Manitoba  
in partial fulfilment of the requirements of the degree of

**Master of Science**

Department of Biological Sciences  
University of Manitoba  
Winnipeg, Manitoba, Canada

Copyright © 2009 Ryan Szajkowski

**THE UNIVERSITY OF MANITOBA  
FACULTY OF GRADUATE STUDIES  
\*\*\*\*\*  
COPYRIGHT PERMISSION**

**Effects of Iron and Oxidative Stress on Cx43 Expression  
and Phosphorylation in Human Enterocytes**

**By**

**Ryan Szajkowski**

**A Thesis/Practicum submitted to the Faculty of Graduate Studies of The University of  
Manitoba in partial fulfillment of the requirement of the degree**

**Of**

**Master of Science**

**Ryan Szajkowski©2009**

**Permission has been granted to the University of Manitoba Libraries to lend a copy of this thesis/practicum, to Library and Archives Canada (LAC) to lend a copy of this thesis/practicum, and to LAC's agent (UMI/ProQuest) to microfilm, sell copies and to publish an abstract of this thesis/practicum.**

**This reproduction or copy of this thesis has been made available by authority of the copyright owner solely for the purpose of private study and research, and may only be reproduced and copied as permitted by copyright laws or with express written authorization from the copyright owner.**

**Table of Contents:**

**PAGE**

<b>Dedication</b>	<b>IV</b>
<b>Acknowledgements</b>	<b>V</b>
<b>Glossary</b>	<b>VI</b>
<b>Abstract</b>	<b>VII</b>

Chapter 1: Literature Review .....	1
1.1 Background: .....	1
1.2 Objectives: .....	3
1.3 Hypothesis: .....	4
1.4 Gastrointestinal Tract: .....	5
1.5 Free Radicals and Oxidative Stress: .....	8
1.6 Disorders of the preterm infant associated with free radicals/oxidative stress: ....	11
1.7 Gap Junctions: .....	13
1.8 Free Radicals and Gap Junctions: .....	15
Chapter 2: Materials & Methods .....	18
2.1 Cells/culture: .....	18
2.2 Milk samples: .....	19
2.3 Semi-quantitative RT-PCR: .....	19
2.4 Real-Time PCR: .....	22
2.5 Western Blot Analysis: .....	23
2.6 Scrapeloading: .....	25
2.7 Transepithelial Electrical Resistance: .....	26
2.8 Immunocytochemistry: .....	27
2.9 Statistical Analysis: .....	27
Chapter 3: Results .....	28
3.1 Iron and Peroxide Modulate Cx43 Transcript Levels: .....	28
3.2 Iron and peroxide modulate Cx43 protein expression and phosphorylation: .....	32
3.3 Immunolocalization of Cx43: .....	38
3.4 Iron and peroxide decrease gap junctional intercellular communication (GJIC): ..	40
3.5 Iron and peroxide decrease transepithelial electrical resistance (TEER): .....	44
Chapter 4: Discussion .....	46
4.1 General outline of this study: .....	46
4.2 Oxidative stress modulates both Cx43 transcript levels as well as protein expression and phosphorylation: .....	47
4.3 Oxidative stress decreases GJIC and TEER across a confluent monolayer: .....	51
4.4 Effect of antioxidant additives on Cx43 gene/protein expression as well as on functional properties of gap junctions: .....	53
4.5 A potential model explaining the effects of oxidative stress on Cx43 gene and protein expression: .....	56
4.6 Oxidative stress and the implications in the human intestine: .....	60

4.7 Summary:.....	61
4.8 Future Directions:.....	62
4.8.1 Theoretical perspective: .....	62
4.8.2 Clinical perspective:.....	64
4.9 Study Limitations:.....	65
Chapter 5: References.....	68

I dedicate this to Camille and to my Mom and Dad.

## *Acknowledgements:*

First, I would like to sincerely thank my Advisor, Dr. Bill Diehl-Jones for his support, patience and guidance during this project. He has been a great mentor and I appreciate everything he has done for me throughout this endeavour.

I would like to thank Dr. Gunnar Valdimarsson and Dr. James Friel for serving on my advisory committee and for their assistance along the way.

I am also grateful to my lab mates Li Yao, Sunjay Lahki and especially Allistair Carrothers for their help; both in the lab and out.

## ***Glossary of Terms:***

BM: Breast milk  
BPD: Bronchopulmonary dysplasia  
Cat: Catalase  
cDNA: Copy deoxyribonucleic acid  
Cx43: Connexin-43  
DMEM: Dulbecco's Modified Eagle Medium  
DNA: Deoxyribonucleic acid  
dNTP: Deoxyribonucleotide triphosphate  
EDTA: ethylenediaminetetraacetic acid  
FBS: Fetal bovine serum  
GI tract: Gastrointestinal tract  
GJIC: Gap junctional intercellular communication  
GPx: Glutathione peroxidase  
GTA: Glycyrrhetic acid  
H<sub>2</sub>O<sub>2</sub>: Hydrogen peroxide  
HGAPDH: Human glyceraldehyde 3-phosphate dehydrogenase  
NEC: Necrotizing enterocolitis  
PBS: Phosphate-buffered saline  
PVDF: polyvinylidene fluoride  
PVL: Periventricular leukomalacia  
RIPA: Radio immunoprecipitation buffer  
RNA: Ribonucleic acid  
ROP: Retinopathy of prematurity  
ROS: Reactive oxygen species  
rRNA: Ribosomal ribonucleic acid  
RT-PCR: Reverse transcriptase polymerase chain reaction  
SOD: Superoxide dismutase  
TBS: Tris-buffered saline  
TEER: Transepithelial electrical resistance  
TPL: Tempol

## ***Abstract:***

Preterm infants, born before 37 weeks gestation, often need breast milk supplementation in order to achieve growth rates comparable to those *in utero*. It has been previously shown that iron supplements in human breast milk increase lipid peroxidation, generate reactive oxygen species (ROS) in cultured enterocytes, and induce apoptosis. Several studies have shown that intracellular ROS alter the expression of gap junction proteins (connexins) and influence gap junctional intercellular communication (GJIC). In the present study, I demonstrate the effects of oxidative stress and iron-supplemented breast milk on the expression and phosphorylation of connexin-43 (Cx43) in the human gut. For these purposes, I have used a well-characterized cell line, CaCo-2BBE, as an *in vitro* model of the intestinal epithelium. Cell cultures were exposed to various dietary factors (including iron) supplemented to human breast milk which have previously been shown to generate intracellular oxidative stress. Cx43 expression was assessed using a number of different molecular biological techniques, including real-time reverse transcriptase polymerase chain reaction (RT-PCR), western blotting and by immunolocalization. GJIC was assessed by dye coupling. Finally, an important function of the intestinal epithelium is to provide a selective permeability barrier. This was assessed by measuring the transepithelial electrical resistance (TEER) across confluent epithelial cell monolayers.

After exposing cells to both peroxide and iron supplemented breast milk treatments, Cx43 gene expression was significantly reduced compared to untreated controls. Interestingly, those same treatments caused a significant increase in overall Cx43 protein expression as well as in the phosphorylated isoform of the protein. Both peroxide and iron caused a decrease in GJIC, with iron showing a dose response. Consistent with other reports in the literature, treatments

which decreased GJIC also decreased TEER suggesting a possible role for gap junctions in maintaining epithelial function.

## ***Chapter 1: Literature Review***

### **1.1 Background:**

According to recent statistics, preterm births represented 7.8% of all live births in Canada as of 2005 (*Statistics Canada*). Preterm infants are often at increased risk for acute illness compared to full-term babies, or those born after 37 weeks gestation. The range of medical complications for which preterm infants are at risk is significant, from both medical resource and human perspectives. The monetary burdens for each day of hospitalization for a preterm infant has generally been estimated to be approximately \$1,500.00/day (Diehl-Jones, *Pers. Comm.*), excluding some of the more specialized medical procedures. Most concerning is the impact of preterm birth and morbidity on these infants, who are very susceptible to the diseases of prematurity and their potentially long-term sequelae. The latter is due, in large measure, to the exposure of preterm infants to increased oxidative stress (1). This is described as an imbalance between oxidant generation and anti-oxidant protection and has been implicated in the pathogenesis of many human diseases (2.).

The reason why oxidative stress is of particular relevance to the neonate is due, in part, to the fact that endogenous defence mechanisms are underdeveloped, and therefore less able to cope with oxidative stress (1). This is exacerbated by the fact that preterm infants are often placed on supplemental oxygen therapy to compensate for their immature respiratory systems (1,3). Recent findings by Laborie et al. have shown that the oxidative imbalance is compounded by the formation of lipid hydroperoxides in unshielded total parenteral nutrition (4). Such research has prompted change in clinical practice aimed at, wherever possible, mitigating sources of oxidative stress.

The foundation for my thesis is that dietary supplements may also induce an imbalance between oxidants and reductants. In order to meet the increased metabolic demands and dietary needs of preterm infants, it is often necessary to add supplements to both maternal breast milk and formulas (5). Supplements such as long chain fatty acids have indeed been shown to increase oxidative stress in enterocytes (6). Of particular relevance in my thesis is the theory that supplemental iron may further exacerbate an oxidative imbalance in the premature infant. The foundation for this theory is laid by Friel et al. who have shown that supplemental iron imposes an additional free radical burden on intestinal epithelial cells (7). Figure 1 represents a simplified model of the neonatal intestinal tract and various sources of reactive oxygen species (ROS) and free radicals mentioned above. As demonstrated in the figure, some of the by-products produced during oxidative metabolism can lead to oxidative stress. Local ischemia/reperfusion injury (as may be caused by a thrombosis) is also depicted. The premise behind my research is that dietary factors, such as iron, further contribute to and exacerbate ROS/free radical formation, and that the neonatal intestine is a particular target for such insult.

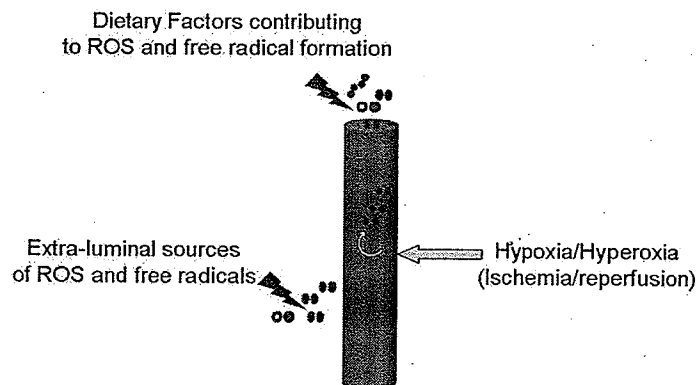


**Figure 1: Potential sources of ROS and free radicals in the preterm infant's gut**

While general cellular damage is accrued as a result of oxidative stress, little is known about the more subtle effects on specific cellular targets. One potential target of oxidative stress is the gap junction, a protein channel that links neighbouring cells together and functions in intercellular communication. Gap junctions are composed of connexin proteins and are found throughout the body in many different isoforms (8). It has been well established that functional gap junctional coupling is important in the maintenance of epithelial functioning (reviewed later). Several studies have demonstrated that oxidative stress affects gap junctions and their functions in other cell types, including cardiac muscle cells and neurons; however, the effects in these tissues are completely different (9,10,11). To my knowledge, there is no literature available on the influence(s) of free radicals on enterocyte gap junctions

## **1.2 Objectives:**

The main objective of my research is to evaluate how intestinal and colonic mucosal cells react to oxidative stress. Specifically, the expression and function of gap junctions when exposed to oxidative stress will be explored. A cell culture model of the human intestine (Caco-2BBE) will be used to test the effects of iron, a commonly used supplement in human breast milk, shown previously to generate intracellular oxidative stress (7). The specific endpoints that will be measured include Cx43 mRNA and protein expression as well as gap junctional intercellular communication (GJIC). Cx43 expression will be assessed using real-time PCR, western blotting and immunolocalization assays. GJIC will be assessed using dye coupling, which quantitatively measures the extent by which cells are coupled by gap junctions. Finally,

another critical function of the intestinal epithelium is to provide a selective permeability barrier. Assessment of this key physiological parameter will be accomplished by measuring transepithelial electrical resistance (TEER) across confluent epithelial cell monolayers.

### **1.3 Hypothesis:**

I hypothesize that iron-induced oxidative stress will modulate Cx43 gene expression and function in Caco-2BBE cells. In turn, this will be manifested by a concurrent decrease in GJIC in the intestinal epithelium, as well as in barrier integrity, as measured by TEER. It is hoped my research will further our understanding of the role(s) of oxidative stress in modulating mucosal physiology and ultimately better enable us to adopt feeding strategies that will reduce enterally-induced oxidative stress and gut dysfunction in the neonate.

With this background, I will review concepts pertinent to this thesis. These include: a brief outline of the gastrointestinal tract with specific focus on the intestinal mucosa; a review of free radical biology and oxidative stress; the molecular structure of gap junctions; and finally the putative effects of oxidative stress on gap junctions.

## **1.4 Gastrointestinal Tract:**

At birth a healthy human gastrointestinal (GI) tract consists of four concentric and functionally different cell layers. The outermost layer, the serosa, consists of several sublayers of epithelial tissue. Deep to these structures is the muscularis externa, which consists of a circular inner smooth muscle layer and a longitudinal outer smooth muscle layer. The coordinated contraction of these 2 sublayers are critical in peristalsis; the action which propels food through the GI tract. The second innermost layer, the submucosa, contains a dense irregular layer of connective tissue with large blood vessels, lymphatics, and nervous tissue. Finally, the intestinal mucosa, the tract's innermost layer, surrounds the lumen or inside of the alimentary canal. It is divided into 3 sublayers of cells; an epithelial layer, the lamina propria and the muscularis mucosae. The muscularis mucosae, the outermost sublayer, is composed of several layers of smooth muscle fibres in a mixed orientation. Contraction of this sublayer renders the mucosa in a constant state of agitation in order to hasten the release of contents from various embedded glands and also to maximize the interaction between the epithelium and the contents of the lumen. The lamina propria is composed of a layer of loose connective tissue and lies beneath the epithelium. In the small intestine, the lamina propria contains capillaries and a central lymph vessel as well as lymphoid tissue. It also contains various exocrine glands with their ducts opening onto the mucosal epithelial layer that release both mucous and serous secretions (12).

The inner most sublayer of the intestinal mucosa is known as the epithelium or mucous membrane. In general, epithelial tissue exists throughout the body in different subtypes. In the small intestine, there are 4 main cell types that comprise the epithelial

layer. The most abundant cell type is the enterocyte, which is critical in digestion and absorption (discussed below). A smaller fraction of the epithelial layer is made up of goblet cells which secrete mucous and have an important role in mucosal protection. Paneth cells are relatively sparse in the small intestine and are involved in immunity. The much rarer enteroendocrine cells secrete various hormones, which chiefly aid in digestion (13). A series of folds called villi characterize the small intestine and serve to increase the surface area of the gut, effectively aiding in the process of digestion and absorption. The apical surface of enterocytes (i.e. the free surface facing the lumen of the intestine) is covered by hundreds of tiny hair-like projections known as microvilli which further increase surface area and therefore the amount of time that luminal contents are exposed to the enterocyte membrane. A glycocalyx coating is present on the apical portion of microvilli which is composed of glycoproteins and is important in digestion and absorption. At the base of each villus the mucosa invaginates downwards to form crypts which range in depth from 0.3mm-0.5mm. Cells of each crypt are involved in mitosis where between 3-6 stem cells continually replicate and divide forcing the daughter cells to migrate upwards. As the cells migrate, they begin to differentiate into one of the cell types discussed previously (14). In the adult, this migratory process occurs very rapidly. Enterocytes are among the most rapidly proliferating cells in the body and have a lifespan of only 3-8 days (15). In the developing fetus, there is a relative timeline by which these cells begin to emerge. At 9 weeks gestation both the enterocytes and goblet cells have fully differentiated. At 11-12 weeks paneth cells are observed at the base of each crypt. At around the same time the enteroendocrine cells become identifiable (16).

The fully differentiated enterocyte, depicted in Figure 2, contains several different junctional proteins important to the cell. Neighbouring cells are held together by several proteins which ultimately serve to build a strong, structural framework (17). Both tight junctions and occluding junctions are located towards the apical surface of enterocytes and are responsible for providing a stringently regulated barrier across the epithelium (18, 19). Desmosomes are intercellular protein junctions along the basolateral portion of the cell that join enterocytes together by binding to the intermediate filaments within the cell membranes of adjoining cells (17). As previously mentioned, gap junctions are proteins that couple cells together and are important for intercellular communication. Recent studies have suggested that they play an important role in barrier function of the mucosa. (20).

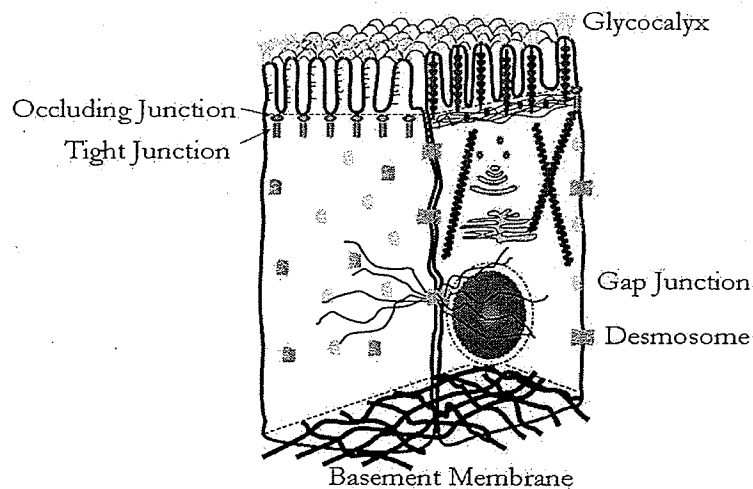


**Figure 2: Schematic representation of a differentiated enterocyte**

The intestinal mucosa has 3 critical functions. It is the first biological barrier in the body, and is vital in keeping unwanted pathogens from entering the body. Further to this is the mucosa's functional immune response to pathogenic bacteria. As the inner most layer of the intestine, the mucosa is the primary surface encountered by nutrients during the process of food digestion and absorption. As a result, the interaction between luminal contents and the mucosa has key implications on intestinal health, integrity, and functioning.

In preterm infants, the situation is somewhat different than described above. The small intestine has not fully developed and as a result of its immature surface, its function is weakened. Infants born before full term are susceptible to an increase in intestinal permeability, a condition known as leaky-gut syndrome. In this case, there is a decrease in the localization and expression of the proteins that make up the aforementioned tight junctions which predisposes the infant's gut to bacterial translocation (21). In preterm infants, the number and length of intestinal villi is much lower than in babies born at full term. Further to this, the number of epithelial cells increases with gestational age and therefore infants born prematurely suffer the consequence of having a decreased surface area in their gut. Consequently, their ability to digest and absorb food nutrients is severely impaired. A decrease in the normal crypt-to-villus cell turnover rate further exacerbates this deficiency (5).

### **1.5 Free Radicals and Oxidative Stress:**

Oxidative stress has been shown to be a contributing factor in the pathogenesis of a multitude of clinical conditions. These include cardiovascular disease, liver disease,

lung disease, neurological disorders and gastrointestinal disease (22). By definition, oxidative stress in the body is caused by reactive oxygen species (ROS). The term ROS does not involve a single entity; rather it can include oxygen ions, peroxides and oxygen free radicals (23). ROS can further be categorized as either one-electron oxidants (radical) or two-electron oxidants (non-radicals) and within each class there exist some that are more reactive and strongly oxidizing than others (23). Generally, due to the presence of unpaired electrons in their outer valence shell, the radical species of ROS are more highly reactive and potentially injurious molecules that can lead to oxidation of various cellular components, including DNA, protein, and lipids (24), and as a result may influence cell proliferation, cell death and the expression of genes (25).

Within cells, ROS are naturally produced at a low, but constant rate as a byproduct of oxygen metabolism (26). Specifically, during oxidative phosphorylation electrons are transported down the electron transfer chain through a series of proteins via redox reactions, with each acceptor protein having a greater reduction potential than the last. The last step of this reaction series involves an electron reaching its last target, a molecule of oxygen which is normally reduced to a water molecule ( $H_2O$ ). However, oxygen can also be reduced to a superoxide radical ( $O_2^-$ ); a highly reactive species (27). Although mitochondrial respiration is probably the most major source of ROS in the body, it can also be produced by ionizing and UV radiation and from the metabolism of a wide spectrum of drugs and xenobiotics (23).

Cells produce several different enzyme scavengers which help to attenuate the effects of ROS in the body. Figure 3 illustrates the mode of action of these

enzymes. Superoxide Dismutase (SOD) catalyzes the disproportionation reaction of a superoxide radical to produce a molecule of oxygen and hydrogen peroxide,  $O_2^- + O_2^- + 2H^+ \rightarrow H_2O_2 + O_2$  (28). While not a radical itself,  $H_2O_2$  is still potentially destructive. Another enzyme, catalase, can then metabolize  $H_2O_2$  into  $H_2O$  and  $O_2$ ,  $2 H_2O_2 \rightarrow 2 H_2O + O_2$  (26,29). Glutathione peroxidases (GPx) are a class of selenoproteins that can also help quench intracellular  $H_2O_2$  by catalyzing its reduction to water and glutathione disulphide from glutathione,  $2GSH + H_2O_2 \rightarrow GS-SG + 2H_2O$  (29,30).

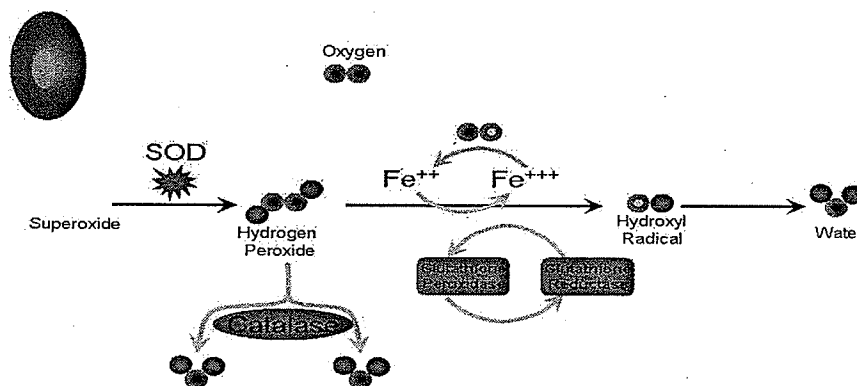


**Figure 3: Schematic flow chart of action of free radical scavengers .**

There exists several other endogenous antioxidants such as ascorbic acid, uric acid and glutathione, which are intrinsically produced through metabolism or retained through diet (25). They stabilize free radicals by donating electrons, which terminates any potential downstream reactions. In doing so, they do not become free radicals, since these species are stable in either form (31).

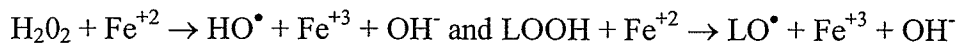
## **1.6 Disorders of the preterm infant associated with free radicals/oxidative stress:**

Oxidative stress has been a problem of particular relevance to the neonate, in whom oxygen free radical damage is believed to contribute significantly to disorders associated with premature birth. In the neonate, innate antioxidant mechanisms are underdeveloped and even relatively low levels of oxidative stress can overwhelm any enzymatic protective response the infant may mount (1). Several studies have supported this by demonstrating that levels of enzyme scavengers increase over the final period of gestation and therefore infants born before full-term have markedly reduced quantities of such protective enzymes (32, 33).

Several illnesses in the pre-term infant, each thought to be caused by the action of ROS have been well documented. For example, Retinopathy of prematurity (ROP) is a vasoproliferative retinal disorder. In newborns, as opposed to adult human beings, the retinal and choroidal circulation is unable to prevent excessive delivery of oxygen to the retina. In the neonate, this combines with the fact that the baby is unable to restrict the production of ROS due to its deficient anti-oxidant defense mechanisms, the result of which can lead to ROP which is the leading cause of visual impairment and blindness (34). Bronchopulmonary dysplasia (BPD) is a chronic lung disease that readily affects preterm infants treated with exogenous oxygen and mechanical ventilation for primary lung disorders. It is thought that BPD begins as an acute inflammation of the lung caused primarily by the toxic effects of ROS (34). Periventricular leukomalacia (PVL) is the predominant form of brain injury in neonates and directly results from ROS injury. It selectively affects cerebral white matter and often evolves into cerebral palsy (35).

When cells of the intestinal mucosa are exposed to oxidative stress in the neonate, the barrier function of the gut may be compromised. A number of different intestinal inflammatory disorders have been attributed to oxidative stress, one of the most notable being necrotizing enterocolitis (NEC) (36). NEC is diagnosed in between 0.9 and 2.4 per 1000 live births and carries a significant mortality rate, ranging from 20-50% (37, 21). It is believed that the production of ROS damages the intestinal epithelium through one of several mechanisms, including disruption of tight junctions (21) and enterocyte apoptosis (34, 38). In either case, this exposes the gut and facilitates entry of various pathogenic bacteria into the body systemically.

In order for preterm infants to achieve optimal growth rates human breast milk is generally not sufficient on its own and is often fortified with various dietary additives, including multivitamins, microlipids and most relevant to my thesis, supplemental iron (6,7). Although iron has many important functions in the body, particularly in oxygen transport, excessive iron levels can be potentially toxic and cause oxidative stress in mucosal cells (7, 39); compounding the internal stress described above. Specifically, it can lead to oxidative stress by generating hydroxyl and alkoxy free radicals through Fenton Chemistry (24):



*HO<sup>•</sup> = hydroxyl radical, LOOH = lipid hydroperoxide and LO<sup>•</sup> = alkoxy radical*

## 1.7 Gap Junctions:

The precise etiology as to how oxidative stress causes disease in the gut is still unclear. One potential target of this stress may be gap junctions, protein channels which facilitate intercellular communication. Figure 4 illustrates a schematic representation of the general structure of gap junctions. In the vertebrate, they are composed of a superfamily of structurally related transmembrane proteins called connexins. Specifically, each gap junction is composed of 2 hemichannels, or connexons which are themselves comprised of 6 connexin proteins. Each connexin protein has intracellular amino and carboxy termini with 4 transmembrane regions that form 2 extracellular loops and 1 intracellular loop (8, 40).

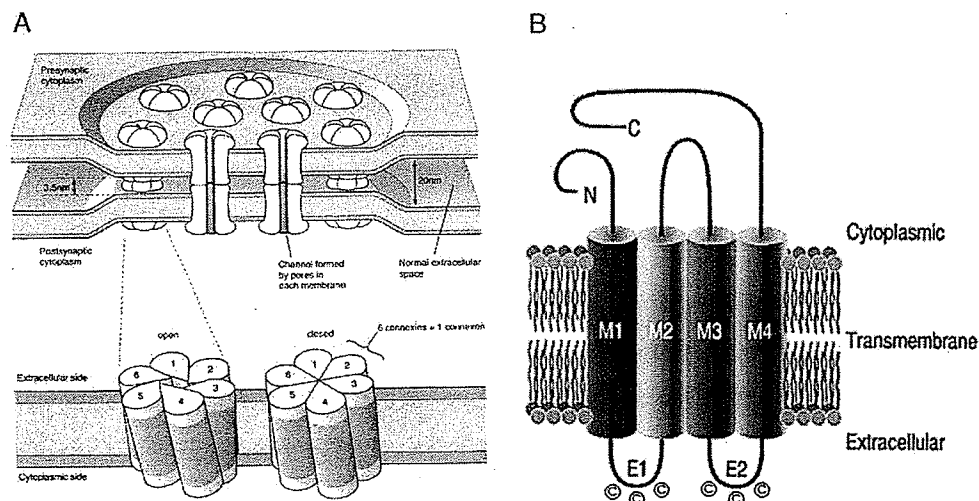


**Figure 4. (A) General schematic representation of gap junctions.**

**(B) Topological model of a connexin protein.**

Taken with permission from Sohl et al. *Gap junctions and the connexin protein family*. Cardiovascular Research, 2004, 62: pp 228-232.

In the human genome there are currently 21 different connexin genes identified (41); the protein products of which weigh in the range of 26-60 kDa and have an average

length of 380 amino acids. There is significant homology between each connexin protein with the greatest diversity occurring in the intracellular loops and carboxy terminal-tail (42).

When 2 hemichannels from different cells directly oppose each other, a fully functional gap junction is formed. Both homomeric and heteromeric gap junctions can be created, which result in different functional properties (41,43). As Figure 5 demonstrates, gap junctions allow neighboring cells to communicate with each other through movements of small molecular mass molecules, ions and second messengers (<1000 Da in size) (42).

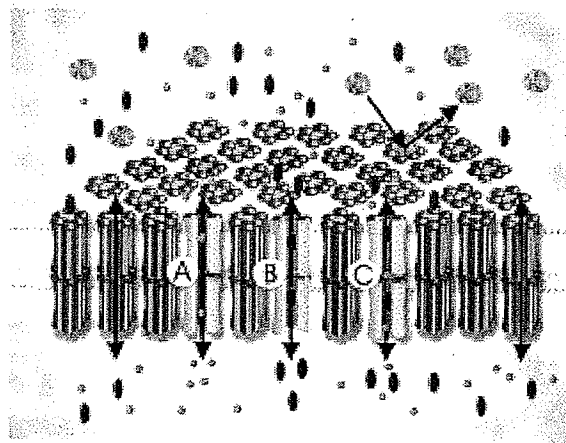


**Figure 5: Schematic drawing illustrating the selective nature of gap junctions in GJIC.**

Taken with permission from Dale W. Laird. *Life cycle of connexins in health and disease.* Journal of Biochemistry, 2006, 394: 527-543.

Cell-to-cell communication is known to be of vital importance in the heart where intercellular communication via gap junctions is critical to the stability of contraction rhythm in the myocardium (44). Expression levels of connexin proteins increase during

the onset of labour and the resultant gap junctions are essential for the development of uterine contractions during this process (45). They are also important in cellular development and differentiation processes (46). During spermatogenesis for instance, germ cell proliferation and differentiation occur through a multi-step sequence of events involving direct intercellular communication through gap junctions (47).

In the human intestine, gap junctions are important in maintaining tissue homeostasis as well as general mucosal health. There is evidence which suggests that GJIC may be directly linked to barrier function. Using a rat model of the stomach, Iwata et al. found that by disrupting GJIC through chemical means, the barrier integrity of the gastric mucosa was compromised (20).

Out of the 21 different connexins in humans, Cx43 is one of the most widely expressed and well-characterized. It exists in several different phosphorylation states with each isoform potentially influencing the functional properties of the gap junction (48).

### **1.8 Free Radicals and Gap Junctions:**

Several studies have been presented which delineate gap junction responses to oxidative stress. In the brain, Frantseva et al. reported that gap junctional coupling mediates the propagation of hypoxic injury to neighboring cells (bystander death) (10). This effect potentiates brain injury and it has been suggested that therapeutic interventions that target specific gap junctions could ameliorate such damage. This finding was confirmed through a study performed by Lin et al., who reported that when cells were oxidatively stressed, protein kinase C gamma (an isoform of PKC found in

neuronal cells and eye tissues) became activated and, in turn, inhibited gap junctions and therefore the spread of any potential damage (49). Another interesting study presented by Lin et al. reported that expression of connexin proteins (not functional gap junctions) is associated with an increased resistance of astrocytes to oxidative stress (50). Because both above processes studied by Lin et al. occur through different mechanisms, it is plausible that both can occur at the same time.

Using cardiac myocytes, Matsushita et al. reported that after inducing hypoxia-reoxygenation, changes in the phosphorylation state as well as distribution of Cx43 were detected (11). These changes in the Cx43 protein might have important implications in cardiac protection. Rakotovaio et al. noted that decoupling of gap junctions during ischemia in the myocardium is associated with Cx43 dephosphorylation and that oxidative stress may be the causative factor (48). Oxidative stress may not only affect coupling status of cells, but also could result in changes to the actual connexin protein (e.g. phosphorylation state), which in turn may influence coupling.

The effects of oxidative stress on gap junctions in the gut are less well understood. Kojima et al. recently reported that connexins are important for maintaining tight junctions in epithelial cells and therefore, may be linked to barrier function (51); although this finding is rather preliminary. It is therefore my main objective to further study the relationship between oxidative stress and gap junctions while looking specifically at Cx43.

For these purposes, I will be using the well-characterized cell line Caco-2BBE, as an *in vitro* model of the intestinal epithelium. Figure 6 is a transmission electron micrograph showing the structure of Caco-2BBE cells (Diehl-Jones, *Pers. Comm.*). This

cell line expresses many important markers unique to the enterocyte, such as retinoic acid binding protein I, retinol binding protein II, and is keratin positive. They also express some of the small intestinal hydrolases, including sucrase-isomaltase, alkaline phosphatase, aminopeptidase N and dipeptidylpeptidase IV. More importantly, Caco-2BBE cells form a polarized monolayer with an apical brush border morphology very close in appearance to the *in vivo* human colon (52). Taken together, the Caco-2BBE cell line is an ideal model for studying the human intestine.

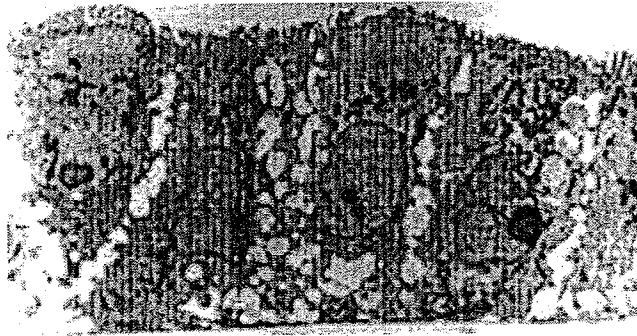


**Figure 6: Transmission electron micrograph of Caco-2BBE Cells grown of polycarbonate filters (10,000 X Magnification)**

## ***Chapter 2: Materials & Methods***

### **2.1 Cells/culture:**

The effects of breast milk (BM), H<sub>2</sub>O<sub>2</sub> and iron on Cx43 gene expression and protein phosphorylation were modeled using CaCo-2BBE cells (ATCC). This cell line is a sub-clone of the well established human colon cancer cell line, CaCo-2, and has become widely-used in studies involving the human intestine because it closely mimics the *in vivo* state. This cell line expresses a brush border similar to both colonic and small intestine cells. Additionally, these cells contain both adult and fetal markers such as villin, fimbrin, sucrase-isomaltase, and myosin I and II (52). Cells were cultured under standard conditions (37 °C, 4.9 % CO<sub>2</sub> and a relative humidity of 80%) in 25 cm<sup>2</sup> cell culture flasks using Dulbecco's Modified Eagle Medium (DMEM) containing glucose (4.5 mg/ml), penicillin (100 U/ml), streptomycin (100 µg/ml), L-glutamine (4mM), human transferrin (10 µg/ml) and 10% fetal bovine system. The medium was changed every 48 hours until a fully-confluent monolayer of cells was reached (approximately 5-7 days). Cell growth was assessed microscopically using the Zeiss Axiovert 200 (Göttingen, Germany). At the point of confluency, the culture medium was removed and the following treatments were added to culture flasks (treatments added were dependant on the experiment performed): BM, BM + 100 µM H<sub>2</sub>O<sub>2</sub>, BM + H<sub>2</sub>O<sub>2</sub> + 350 units/ml Superoxide Dismutase (SOD), BM + H<sub>2</sub>O<sub>2</sub> + 150 units/ml Catalase (Cat), BM + 0.3 mM Fe<sup>+2</sup>, BM + 0.9 mM Fe<sup>+2</sup>, BM + 1.8 mM Fe<sup>+2</sup>, BM + 1.8 mM Fe<sup>+2</sup> + SOD, BM + 1.8 mM + Cat and BM + 1.8 mM Fe<sup>+2</sup> + 10 mM Tempol. Cells were incubated at 37°C for a pre-determined period of time, dependant on the assay performed (see results). The treatments were then removed and the cells were thoroughly, but carefully washed with

either fresh culture media or PBS. To detach cells from the substrate, 1 ml of sterile EDTA (0.02%) was added to chelate all residual calcium for 1 minute before being removed. This was followed by the addition of another 1 ml of EDTA (0.02%) and 1.5 mls of trypsin (0.25%) and cells were incubated in this state for approximately 15 minutes or until cells started to visibly become detached from the flask. At this point, fresh medium containing fetal bovine serum (FBS) was then added; this inhibited the action of trypsin. Detached cells were transferred to a sterile 15 ml Falcon® tube and centrifuged at 250 g's for 5 minutes. The resulting supernatant was aspirated and the cell pellet was resuspended in 1.5 mls of culture media and transferred to a sterile 1.5 ml microcentrifuge tube. Cells were then centrifuged at 2000 g's for a further 5 minutes with the supernatant again removed. Cell pellets were then stored at -86 °C until ready to proceed with experimentation.

## **2.2 Milk samples:**

Breast milk was collected with appropriate consent and ethical approval (NREB, U of M) from women who delivered infants between 29 and 34 weeks gestation at St. Boniface General Hospital. Breast milk was pooled from 3 different women and the resultant milk samples were immediately aliquoted in 50 ml vessels and stored at -86°C.

## **2.3 Semi-quantitative RT-PCR:**

Total RNA was extracted from cell pellets using Trizol reagent (Invitrogen, Carlsbad, Ca) according to the manufacturer's instructions. Briefly, cells were

homogenized in 1 ml of Trizol reagent using a power homogenizer (Mandel-Kontes, Vineland, NJ) and allowed to incubate at room temperature for 5 min to allow for the complete break-down of the nucleoprotein complex. To separate RNA from DNA and protein, 0.2 ml of chloroform was added and each tube was shaken vigorously for 15 seconds and subsequently allowed to incubate for a further 3 minutes at room temperature. Samples were then centrifuged at 12,000 g's for 15 minutes at 4 °C which resulted in the separation of a lower phenol-chloroform phase, an interphase and a colorless upper aqueous phase exclusively containing the RNA of interest. The aqueous phase was transferred to a fresh tube and precipitated using 0.5 ml of isopropyl alcohol for 10 minutes and was again centrifuged at 12,000 g's for another 10 minutes. The RNA precipitate was washed once with 75% ethanol and stored at -86 °C until ready to proceed with DNase treatment.

DNase treatment was performed on each RNA sample using the Turbo DNA-free kit (Ambion, Austin, TX). The RNA pellets were air-dried for approximately 30 minutes before being re-suspended in 17 µl of DEPC-treated water. 1 µl of RNase Out inhibitor and 2 µl of Turbo DNase buffer was added to each sample which was mixed gently before addition of 1 µl of Turbo DNase. Samples were incubated at 37 °C for 30 minutes at which point 2 µl of DNase inactivation reagent was added and allowed to incubate for a further 3 minutes at room temperature. The samples were then centrifuged at 12,000 g's rpm for 2 minutes and the resulting supernatant (pure RNA) was carefully removed and put into a fresh microcentrifuge tube. The quality and quantity of RNA was determined using spectrophotometrical measurements at 260 and 280 nm (Ultraspec 3100 pro, Biochrom Ltd., Cambridge, England). All samples studied had a  $A_{260}/A_{280}$

ratio of >2.00.

First strand cDNA was synthesized using 3 µg total RNA which was initially added to 1 µl dNTP's (10mM) and 2 µl random hexamers with the volume being brought up to 12 µl with PCR grade water. This was heated at 65 °C for 5 minutes and then a master mix containing 4 µl 5X first strand buffer (250 mM Tris-HCL, 375 mM KCl, 15 mM MgCl<sub>2</sub>), 2 µl DTT (0.1 M) and 1 µl RNase out was added to each sample which was again heated at 42 °C for 2 minutes. 1 µl of Superscript II (Invitrogen) was then added and the mixture heated at 42 °C for 50 minutes and inactivated by heating to 70 °C for a final 15 minutes. Semi-quantitative multiplex PCR reactions were carried out using 18S rRNA as an internal standard (Quantum RNA Classic 18S kit, Ambion). After determining the linear range for Cx43 (i.e. the number of cycles in the linear range) and experimentally verifying the optimal ratio of 18S Primers:Competimers, each PCR mixture was set up as follows: 2 µl of cDNA, 2 µl of PCR reaction buffer, 0.4 µl of dNTP's (10 mM), 0.8 µl of Cx43 primer pair (5 µM), 0.8 µl of 18S: primer:competimer mixture (5 µM), 0.6 µl of MgCl<sub>2</sub> and 0.2 µl of Taq DNA polymerase all in a total volume of 20 µl per reaction. The following primer pair was used:

**Cx43 primers:** Forward: GCACCATCTCTAACTCCCATGCAC  
Reverse: GAATAAGGCTGTTGAGTACCACCTCC

The cDNA template was initially denatured by heating to 94°C for 3 minutes and amplified by 33 cycles (optimal) of 94°C for 45 seconds, 65°C for 45 seconds and 72°C for 60 seconds. A final elongation step at 72°C for 7 minutes was performed. PCR products were separated on a 1.5% agarose gel and stained using SYBR green (Molecular Probes, Eugene, OR). Gels were photographed (Sony, model XCD-X700, Northern

Eclipse software) using an ultraviolet transilluminator at 302 nm (Ultraviolet products, model TFM-20).

## **2.4 Real-Time PCR:**

In order to confirm and validate the data found from the semi-quantitative PCR method (above), real-time PCR was also performed. The cDNA was prepared in the same way as described above (for the semi-quantitative method). In order to determine the correct amount of cDNA template to use for each reaction it is important that gene amplification fits within the linear (or exponential range) of the curve. To make this distinction, three 10-fold dilutions of the cDNA were prepared (1:1, 1:10, 1:100, 1:1000) and an initial calibration quantitative PCR (qPCR) was set up. Each 20 µl reaction contained the following: 10 µl iQ SYBR Green Supermix, 1 µl forward primer (10 µM stock), 1 µl reverse primer (10 µM stock), 7 µl sterile PCR grade water, 1 µl cDNA template. With 1 of my samples I loaded the above qPCR into a 96-well plate using the IQ5 Real-time detection system (Bio-Rad, Hercules, CA) according to manufacturer's instructions. Primers against human glyceraldehyde 3-phosphate dehydrogenase (the internal standard) and primers for Cx43 (gene of interest) were used (Sigma-Aldrich Oakville, On). Each reaction was set up in triplicate to improve validity.

**HGAPDH primers:** Forward: AACTTTGGTATCGTGGAAGG  
Reverse: CAGTAGAGGCAGGGATGATGT

**HCx43 primers:** Forward: CAATCACTTGGCGTGACTTC  
Reverse: GTTTGGGCAACCTTGAGTTC

The cDNA template was initially denatured by heating to 95 °C for 3 minutes and amplified by 40 cycles of 95 °C for 10 seconds and 60 °C for 30 seconds. At the end of cycle 40, the program was designed to include a melt-curve analysis in order to test for DNA purity and to guard against any contamination. After analyzing the data, the standards that were set up (i.e. HGAPDH) were translated into a standard curve. From it, the maximum and minimum amount of template to use was determined. The appropriate dilutions that fit on the standard curve within that range were chosen with each reaction performed thereafter. From the initial calibration, it was discovered that Cx43 is a relatively low-expressing gene compared to HGAPDH. To account for this difference, it was necessary to use a 1:10 dilution of cDNA with the HGAPDH primers and a 1:1 ratio (i.e. pure cDNA) with the Cx43 primers. These were the dilutions of cDNA template used for all subsequent qPCR experiments. The data were analyzed using a comparative cycle threshold method with the dilution factors being taken into account (Applied Biosystems).

## **2.5 Western Blot Analysis:**

Cell lysates were prepared by resuspending cell pellets in RIPA buffer (50 mM Tris-HCL, 150 mM NaCl, 0.1% SDS, 0.5% sodium deoxycholate, 1% Triton X-100, pH 8.0) containing a protease inhibitor cocktail which included 500 µM 4-(2-Aminoethyl) benzenesulfonyl fluoride hydrochloride, 150 nM Aprotinin, 1 µM E-64, 0.5 mM EDTA, Disodium, 1 µM Leupeptin, Hemisulfate (Calbiochem). Phosphatase inhibitors [sodium orthovanadate (1 mM) and sodium fluoride (25 mM)] were also added. Protein concentrations were measured colorimetrically using the BSA Protein Assay Kit (Pierce,

Rockford, Il.). At this point, all protein samples were stored at -86 °C until ready to proceed. Equal protein concentrations (25 µg) were prepared using RIPA buffer as a diluent and these samples were boiled for 5 minutes to denature any protein aggregates that may have formed. The samples were then cooled to room temperature and centrifuged at 2000 G's before loading into their appropriate lanes. They were then separated on a 10% polyacrylamide denaturing gel (1.5 M Tris-HCL, 10% SDS, Acrylamide/Bis-30%T, 10% Ammonium persulfate, 0.05% TEMED) at a voltage of 150 volts for approximately 60 minutes (or until the dye fronts had run at least ¾ down the gel). This was followed by transfer to polyvinylidene fluoride (Millipore Bedford, MA) membranes at an amperage of 200 mAmps for 1.5 hours to ensure complete transfer of protein. Membranes were subsequently blocked using 3% BSA in Tris-buffered saline (TBS)/0.5% Tween 20 for at least 1 hour. This was followed by addition of primary antibody (Sigma-Aldrich Oakville, On.) against Cx43 (1:4000 in TBS/0.1%Tween 20) at 4°C overnight. The membranes were then incubated at 37 °C for 60 minutes at which point the primary antibody was removed and each blot was thoroughly washed in TBS/0.1%Tween 20 (4X). Anti-rabbit IgG peroxidase conjugate (Sigma-Aldrich Oakville, On.) was then added at a concentration of 1:8000 (in TBS/0.1%Tween 20) and was allowed to incubate for 2 hours at 37 °C. Another round of extensive washing was performed and the binding was detected using a chemiluminescence system (Supersignal; Pierce Rockford, Il.) and X-ray film (Kodax BioMax Light Film; Sigma-Aldrich Oakville, On.) using standard developing protocols.

To assess the native phosphorylation state of Cx43, confluent Caco-2BBE cells (untreated) were harvested as usual. With one of the cell pellets, the cell lysate was

prepared exactly as described above. With another pellet, cells were resuspended in RIPA buffer containing the aforementioned protease inhibitors with the phosphatase inhibitors omitted. A dephosphorylation buffer (0.5 mM Tris-HCL, 1 mM EDTA, pH8.5) was added followed by the addition of calf intestinal alkaline phosphatase (Promega, Madison, WI). The lysate was incubated at 37 °C for 8 hours followed by addition of RIPA buffer. Samples were then boiled for 5 minutes before being frozen at -86 °C. Western blot analysis was performed in the same manner as described above and a comparison of Cx43 protein was made between the phosphatase-treated cells and non-treated cells.

## **2.6 Scrapeloading:**

CaCo-2BBE cells were grown to confluency on 35-mm sterile petri plates pre-coated with a 2.5% Matrigel® solution (BD Biosciences, Bedford MA), a basement membrane matrix which promotes cellular adhesion and differentiation. BM treatments were added following the removal of medium and incubated for 1.5 hours. Controls using 100 µM glycyrrhetic acid (GTA) were incubated for 24 hours to induce complete decoupling of gap junctions. Following extensive washes with PBS (pH 7.4), a 0.1% Lucifer Yellow and 1% Rhodamine Red-Dextran solution was added to the cells. Monolayers were then scraped using a microscalpel and allowed to incubate for 10 minutes. Cells were again washed and fixed with 4% paraformaldehyde. Gap junctional intercellular coupling (GJIC) was assessed using fluorescence microscopy (Zeiss Axioskop microscope with epifluorescence optics, Sony Power HAD 3CCD colour video

camera). Along each scrape-line, three points were arbitrarily chosen and the number of contiguously labelled cells were counted and averaged.

## **2.7 Transepithelial Electrical Resistance:**

CaCo-2BBE cells were plated onto polycarbonate membranes with 0.4  $\mu\text{m}$  pore size in 4mm diameter Transwell® chambers (Corning Incorporated, NY) pre-coated with a 2.5% Matrigel® solution (BD Biosciences, Bedford MA). Cells were grown to confluency (14-21 days). Measurements of transmembrane electrical resistance (TEER) were made using the WPI REMS Autosampler (Sarasota, FL.). The measurements were taken by placing the longer electrode into the basal lateral media and the shorter electrode into the apical media. TEER was measured in a control well which was void of any cells, enabling us to measure the resistance provided by the Transwell® inserts. This value was subtracted from all subsequent sample readings. After stable TEER measurements between 500-600 Ohms were taken (indicative of a confluent monolayer), culture medium was aspirated and 50  $\mu\text{l}$  of the appropriate breast milk treatment was added to the apical compartment of the Transwell® chamber and incubated for 3 hours at 37°C. Control wells with 100  $\mu\text{M}$  GTA were incubated for 24 hours to induce decoupling of gap junctions. Apical chambers were then aspirated and carefully washed three times with fresh culture medium. Endpoint TEER measurements were taken with rinse steps using sterile media between each measurement. This served to reduce mixing of components from one chamber into another. Final TEER values were recorded and any changes in TEER were calculated.

## **2.8 Immunocytochemistry:**

CaCo-2BBE cells were grown to confluency (3-5 days) on glass cover slips coated with a 2.5% Matrigel® solution (BD Biosciences Bedford MA). Cells were then fixed and permeabilized with ice-cold methanol:acetone (50:50) for 1 minute after which they were washed in PBS (pH 7.4) three times then blocked with 1% BSA in PBS for approximately 1 hour. Coverslips were then incubated overnight at 4°C with primary antibody (1:400 dilution) against Cx43 (Sigma Aldrich, Oakville, On.), followed by a 1 hour incubation at 37°C. Coverslips were then washed three times with PBS before addition of the secondary antibody (1:400-Goat anti-rabbit-Alexa-568 from Molecular Probes, Eugene, OR). A nuclear Hoescht stain (1 µg/ml) was added along with the secondary antibody. The coverslips were incubated for 1 hour at 37°C, then washed and mounted in TBS/glycerol (50:50). A negative control was also included in which the secondary antibody was omitted. Fluorescence microscopy was performed using the Zeiss Photo II microscope with epifluorescence optics (Hamamatsu Orca cooled CCD digital camera-Bridgewater, NJ).

## **2.9 Statistical Analysis:**

For each assay (where applicable), a one-way analysis of variance (ANOVA) with the Tukey post hoc test to describe the relationship between means was used.  $P < 0.05$  was considered to be statically significant. N-values varied between assays, with a minimum value of 2 being used in each case.

## ***Chapter 3: Results***

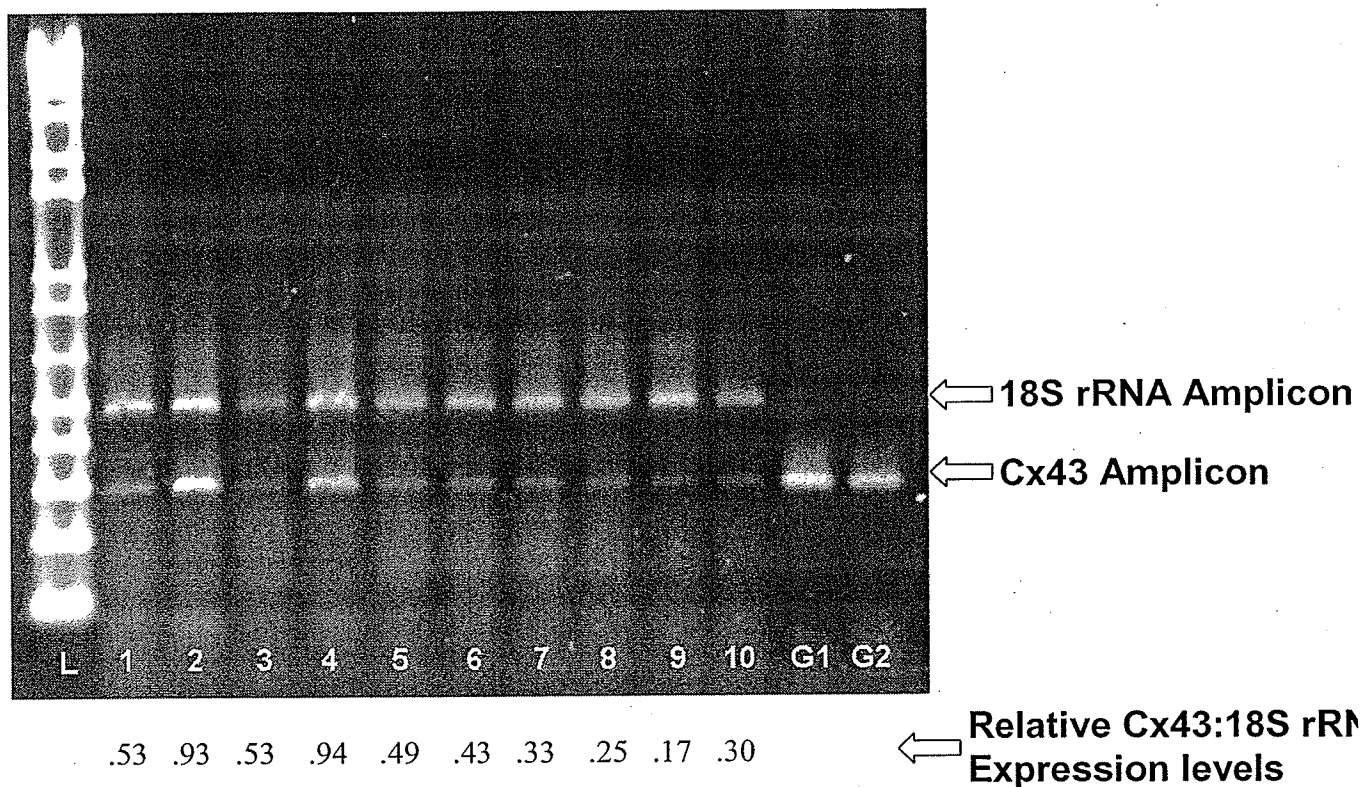
### **3.1 Iron and Peroxide Modulate Cx43 Transcript Levels:**

To measure Cx43 gene expression, a semi-quantitative PCR approach was employed. Briefly, Caco-2BBE cells were grown to confluency on 25cm<sup>2</sup> cell culture flasks and the following treatments were added: culture medium (control), breast milk (BM), BM + 100  $\mu$ M H<sub>2</sub>O<sub>2</sub>, BM + H<sub>2</sub>O<sub>2</sub> + 350 units/ml Superoxide Dismutase (SOD), BM + H<sub>2</sub>O<sub>2</sub> + 150 units/ml Catalase (Cat), BM + 0.3 mM iron Fe<sup>+2</sup>, BM + 0.9 mM Fe<sup>+2</sup>, BM + 1.8 mM Fe<sup>+2</sup>, BM + 1.8 mM Fe<sup>+2</sup> + SOD, BM + 1.8 mM Fe<sup>+2</sup> + Cat. After a 2 hour incubation period at 37 °C and 80% relative humidity, cells were trypsinized and pelleted into 1.5 ml RNase-free microtubes. Total RNA was extracted using Trizol reagent according to manufacturer's instructions. First strand cDNA was synthesized using 3 $\mu$ g of DNase-treated RNA after which semi-quantitative multiplex PCR reactions were carried out using 18sRNA as an internal standard. PCR products were separated on a 1.5% agarose gel and stained using SYBR green. Gels were then photographed using an ultraviolet transilluminator.

As Figure 7 illustrates, typically two distinct bands appeared in each lane. The upper band corresponds to the 18s rRNA amplicon while the lower band corresponds to the Cx43 amplicon; based on marker size. Through line-scan densitometry, relative Cx43 expression levels could be assessed within each sample and then compared back to the untreated control to gain some understanding of how these individual treatments affected Cx43 gene expression. In breast milk treated cells, Cx43 gene expression was drastically increased (75%). When H<sub>2</sub>O<sub>2</sub> was added in conjunction with BM, no change in Cx43 expression was detected. Interestingly, when SOD and catalase were added with

BM + H<sub>2</sub>O<sub>2</sub> opposing effects were observed, with SOD significantly increasing Cx43 expression (77%) and catalase decreasing Cx43 expression (8%). When iron was added in conjunction with BM, Cx43 gene expression decreased in a dose-dependant manner with 0.3 mM Fe<sup>+2</sup> decreasing expression by 19%, 0.9 mM Fe<sup>+2</sup> by 38% and 1.8 mM Fe<sup>+2</sup> by 53%. When SOD was added to BM + 1.8 mM Fe<sup>+2</sup> a further decrease in Cx43 expression of 68% was noted. Catalase slightly restored expression levels compared to BM + 1.8 mM Fe<sup>+2</sup> alone with a decrease of only 43%.

**Figure 7: A semi-quantitative analysis of the effects of various breast milk treatments on Cx43 gene expression**



**Legend:** L = Ladder; 1 = culture medium; 2 = BM; 3 = BM/H<sub>2</sub>O<sub>2</sub>; 4 = BM/H<sub>2</sub>O<sub>2</sub> + SOD; 5 = BM/H<sub>2</sub>O<sub>2</sub>/Cat; 6 = BM + 0.3 mM Fe<sup>+2</sup>; 7 = BM + 0.9 mM Fe<sup>+2</sup>; 8 = BM + 1.8 mM Fe<sup>+2</sup>; 9 = BM + 1.8 mM Fe<sup>+2</sup>/SOD; 10 = BM + 1.8 mM Fe<sup>+2</sup>/Cat; G1/G2 CaCo-2<sub>BBE</sub> Genomic DNA

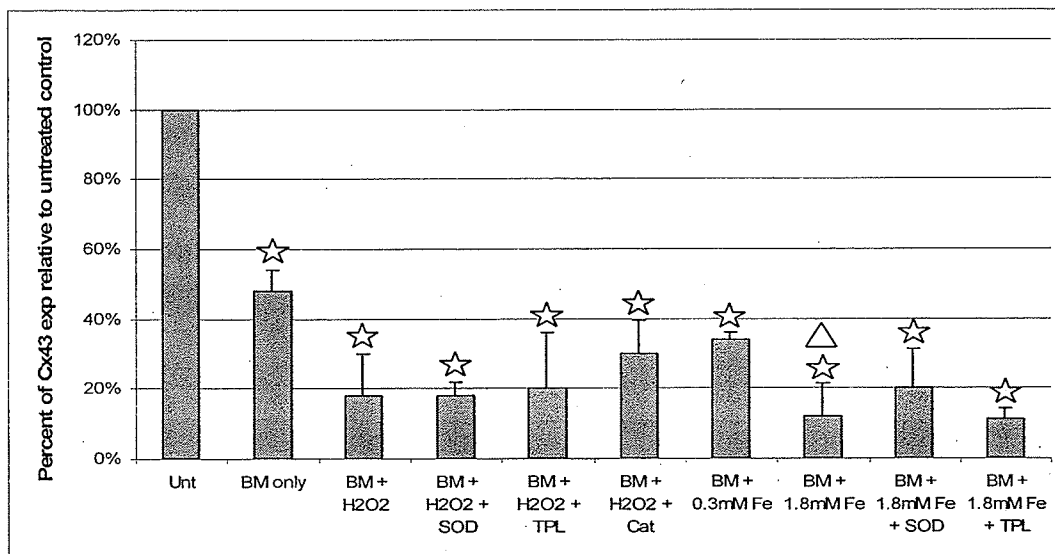
Given that this analysis provided only a semi-quantitative measure of Cx43 expression, to confirm these results, real-time PCR (also known as qPCR) was performed. The benefit to using this technique is that it amplifies and simultaneously quantifies Cx43 mRNA transcripts, giving a more accurate and precise assessment of Cx43 gene expression levels. Briefly, Caco-2BBE cells were grown to confluency on 25cm<sup>2</sup> cell culture flasks and the following treatments were added: culture medium (control), breast milk (BM), BM + 100  $\mu$ m H<sub>2</sub>O<sub>2</sub>, BM + H<sub>2</sub>O<sub>2</sub> + 350 units/ml Superoxide Dismutase (SOD), BM + H<sub>2</sub>O<sub>2</sub> + 150 units/ml Catalase (Cat), BM + H<sub>2</sub>O<sub>2</sub> + 10 mM Tempol (TPL), BM + 0.3 mM iron Fe<sup>+2</sup>, BM + 1.8 mM Fe<sup>+2</sup>, BM + 1.8 mM Fe<sup>+2</sup> + SOD, BM + 1.8 mM + Cat, BM + 1.8 mM Fe<sup>+2</sup> + TPL. Treatments were incubated for 2 hours at 37 °C and 80% relative humidity at which point total RNA was extracted and reverse-transcribed in the same manner as described above (for semi-quantitative PCR). After determining the correct dilutions of cDNA template to use, qPCR reactions were carried out and the data analyzed using a comparative cycle threshold method.

According to this analysis, there was a 52% decrease in Cx43 expression in breast-milk treated cells (Figure 8); which is inconsistent with the semi-quantitative result which demonstrated a 75% increase in expression (from above). When H<sub>2</sub>O<sub>2</sub> was added in combination with breast milk, an 82% decrease Cx43 expression was noted. Each of the scavengers, SOD, tempol and catalase did little to restore Cx43 expression levels with catalase having the greatest impact where expression levels had only decreased to 70% relative to untreated controls. Each of the aforementioned results involving H<sub>2</sub>O<sub>2</sub> conflicted with the corresponding data from the semi-quantitative analysis. This

discrepancy can likely be explained by the fact that the H<sub>2</sub>O<sub>2</sub> in the former case was old and concentrations were therefore inaccurate. When low concentrations of iron (0.3 mM) were added in conjunction with breast milk, a 66% decrease in Cx43 expression was detected. When high iron concentrations were added (1.8 mM) an 88% reduction was noted. Interestingly, this same trend involving iron treatments was found in the semi-quantitative analysis from above. When SOD and tempol were added with high iron concentrations, a minimal restorative effect on Cx43 expression was detected, with SOD having a slightly greater effect (80% decrease relative to control).

To test the significance of iron alone on Cx43 gene expression, a statistical comparison between the BM and the BM + 1.8 mM Fe<sup>+2</sup> treatments was also made. Cx43 gene expression in BM + 1.8 mM Fe<sup>+2</sup> treated cells was 36% lower than in BM treated cells, but this finding was only significant at an adjusted confidence level of 85%.

**Figure 8: A quantitative analysis of the effects of various breast milk treatments on Cx43 gene expression**



Data shown as mean +/- SEM (N=2). ☆ symbol signifies statistically-significant differences compared to untreated control (p < 0.05). △ symbol signifies statistically-significant differences compared to BM only treatment (p < 0.15).

### **3.2 Iron and peroxide modulate Cx43 protein expression and phosphorylation:**

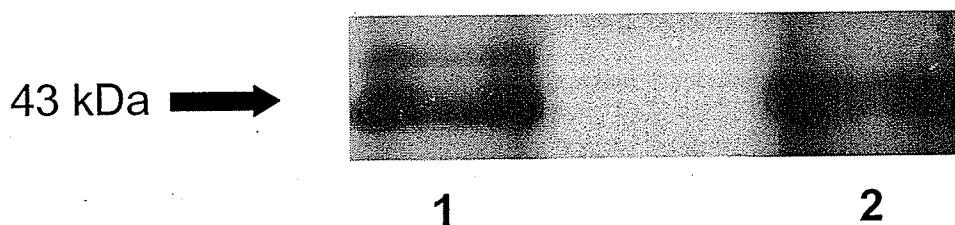
To measure Cx43 protein expression levels as well as potential differences in the phosphorylation state of Cx43, the western blot technique was performed. Briefly, Caco-2BBE cells were grown to confluency on 25cm<sup>2</sup> cell culture flasks and the following treatments were added: culture medium (control), breast milk (BM), BM + 100 μm H<sub>2</sub>O<sub>2</sub>, BM + 1.8 mM Fe<sup>+2</sup>, BM + 1.8 mM Fe<sup>+2</sup>+ SOD, BM + 1.8 mM Fe<sup>+2</sup> + 10 mM Tempol (TPL). After a 2 hour incubation period, cells were trypsinized and pelleted into 1.5 ml RNase-free microtubes. Cell lysates were prepared by resuspending cell pellets in RIPA buffer containing a protease inhibitor cocktail and phosphatase inhibitors [sodium orthovanadate (1 mM) and sodium fluoride (25 mM)]. Protein concentrations were quantified using the BCA Protein Assay kit. Equal protein concentrations (25 μg) were then separated on a 10% polyacrylamide denaturing gel followed by transfer to polyvinylidene fluoride (PVDF) membranes. Membranes were then blocked with 3% Bovine Serum Albumin (BSA), 0.5% Tween-20 in Tris-buffered saline and incubated with primary antibody against Cx43 at 4°C overnight. Anti-rabbit IgG peroxidase conjugate was added following extensive washes. Binding was detected using a chemiluminescent system and the blots were transferred to X-ray film using standard developing procedures. For all blots, a pre-stained protein ladder was included to ensure that the protein bands observed were of the expected size (i.e. 43 kDa).

To analyze the data, line-scan densitometry (Northern Eclipse software) was performed on each band which allowed for a quantitative measurement of Cx43 protein expression. When doublets or triplets were detected, each band was assessed individually

thereby enabling me to calculate differences in the phosphorylation state between samples.

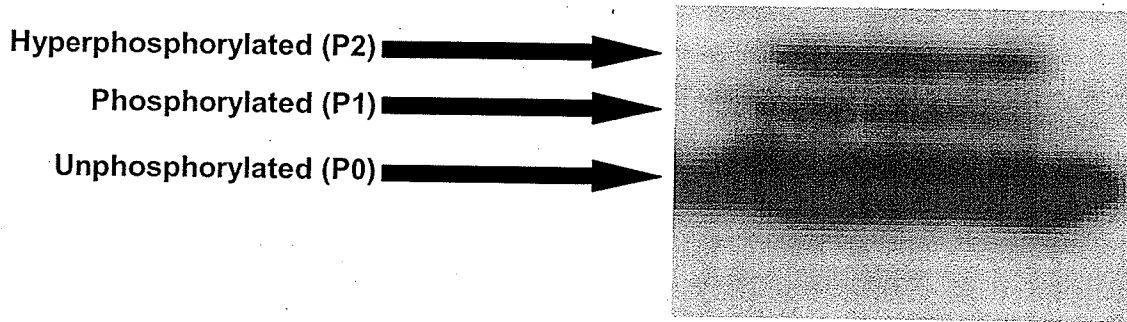
Initially, it was important to assess the native phosphorylation state and migration pattern of Cx43 in Caco-2BBE cells since this has not been published before. In order to do so, two untreated samples of Caco-2BBE cells were harvested as usual. From Figure 9, the protein lysate in lane 1 was prepared in exactly the same manner as described above with the phosphatase inhibitors included. The protein lysate in lane 2 was dephosphorylated with alkaline phosphatase before electrophoresis. A western blot was performed (as described above) with the two samples run side-by-side to distinguish any differences in the phosphorylation pattern of Cx43. In this case, a 12% polyacrylamide gel was used in order to achieve better separation of Cx43 isoforms. As Figure 9 demonstrates, a single molecular weight band of 43 kDa was detected in lane 2 (the phosphatase treated sample), while a doublet was observed in lane 1 (phosphatase inhibitors included); the lower band in the 43 kDa range and the upper being approximately 45kDa.

**Figure 9: Changes in Cx43 migration is due to Phosphorylation**



From these results, the native phosphorylation state of Cx43 can be described by the following figure:

**Figure 10: Native phosphorylation state of Cx43**



Having elucidated the native phosphorylation state of Cx43, a western blot was performed using cell lysates from the samples described above. Figure 11 is a representative western blot from one of the trials performed. According to Figure 12 below, when cells were treated with breast milk alone there was a marginal increase in Cx43 expression of both the phosphorylated and unphosphorylated isoforms when compared to the untreated control (35% and 6% respectively), but these differences were not statistically significant. When BM and peroxide were added to cells a significant increase in the phosphorylated isoform of 122% was observed, while an insignificant increase of 10% was detected in the unphosphorylated isoform. When cells were treated with BM and high iron concentrations the phosphorylated isoform of Cx43 was increased considerably by 199% while the unphosphorylated form increased by only 40%. Interestingly, when the free radical scavenger Tempol was added it did not restore Cx43 expression levels, and in fact a further increase of the phosphorylated form was noted

(213% compared to the control). Expression of the unphosphorylated isoform was increased by only 31%.

To test the significance of iron alone on Cx43 protein expression, a comparison was made between the BM and BM + 1.8mM Fe<sup>+2</sup> treatments. The latter treatment was found to significantly increase both the phosphorylated and unphosphorylated isoforms of the Cx43 protein (164% and 34% respectively) relative to BM alone (95% confidence level).

**Figure 11: Western blot showing differences in Cx43 protein expression and phosphorylation**

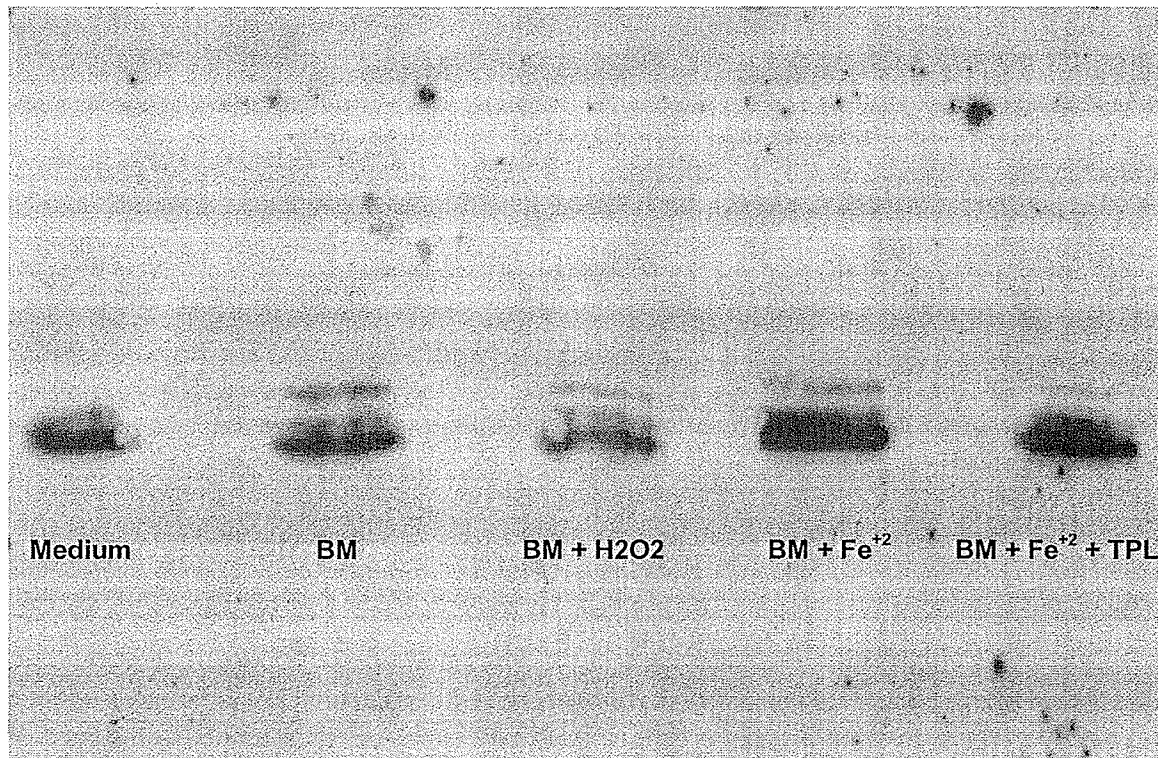
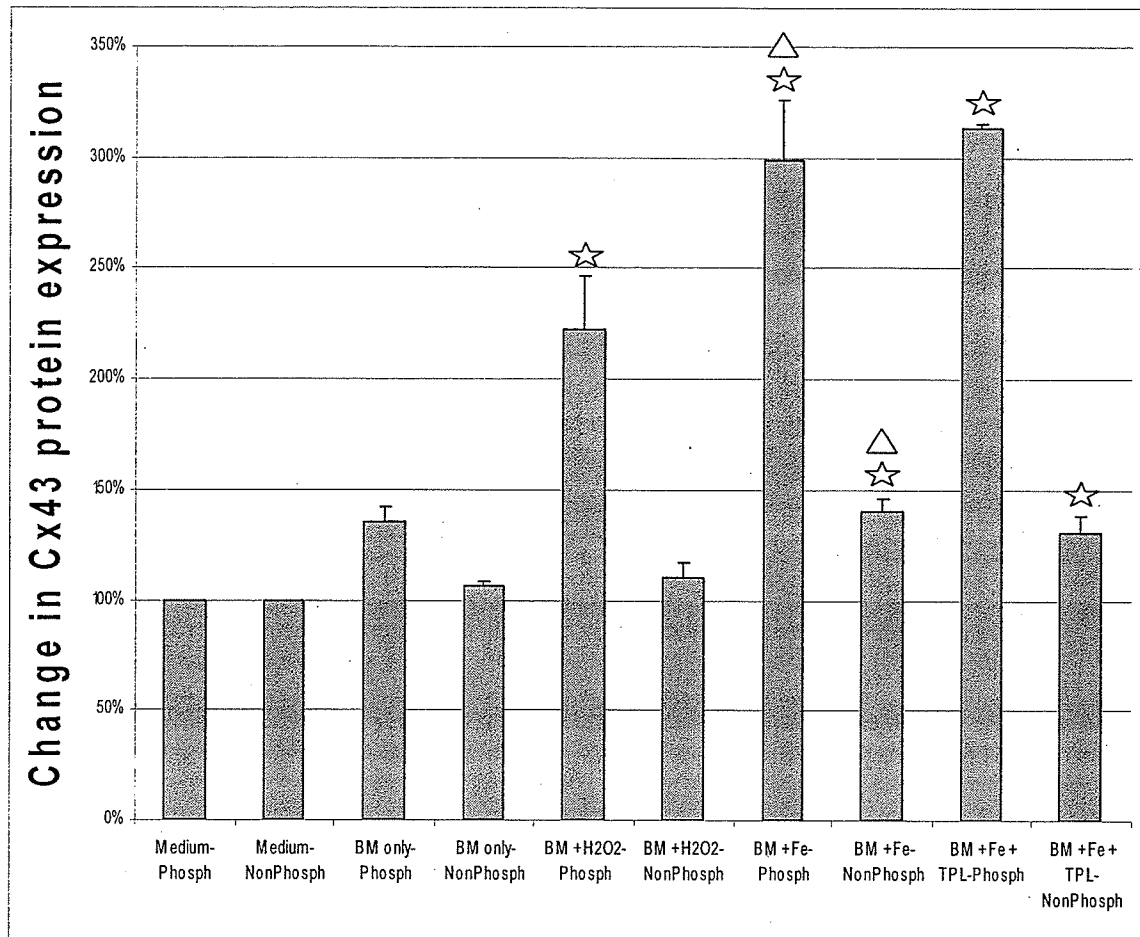


**Figure 12: A quantitative analysis of the effects of various breast milk treatments on Cx43 protein expression**



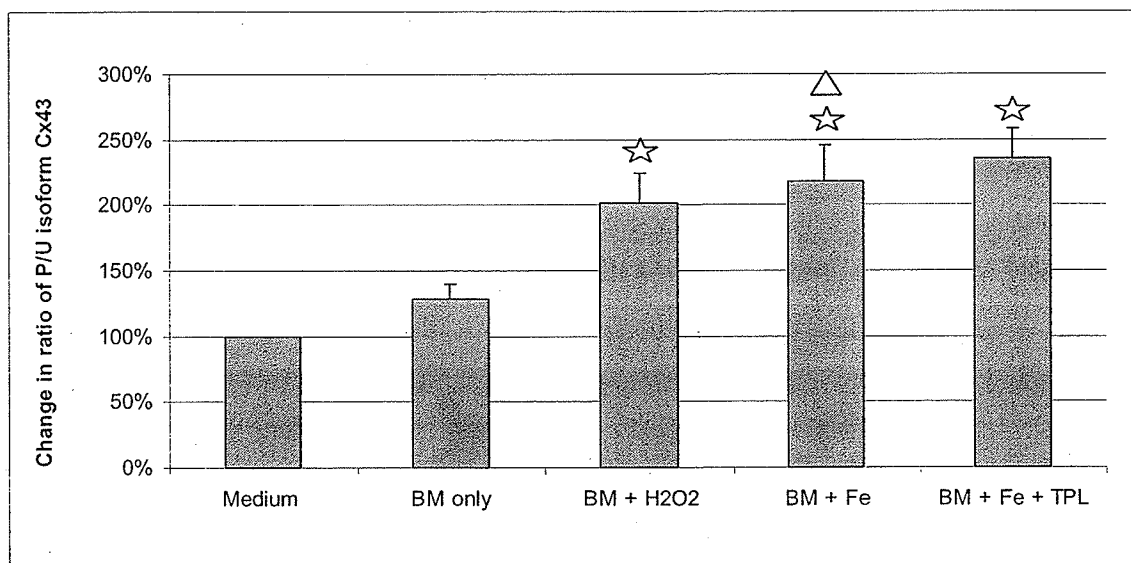
Data shown as mean +/- SEM (N=3). ☆ symbol signifies statistically-significant differences compared to untreated control ( $p < 0.05$ ). △ symbol signifies statistically-significant differences compared to BM only treatment ( $p < 0.05$ ).

To gain a better understanding of how the above treatments specifically affect phosphorylation of Cx43 the change to the ratio of the phosphorylated to unphosphorylated (P/U) isoforms was calculated. As demonstrated in Figure 13, when cells were treated with breast milk the P/U ratio was increased by 29% when compared to untreated controls. In BM and peroxide-treated cells the ratio was considerably increased

to 102% of that of the controls. When cells were treated with BM and high iron concentrations a further increase of 118% was observed. Interestingly, when tempol was added the P/U ratio was further increased to 136%.

After comparing the BM and the BM + 1.8mM + Fe<sup>+2</sup> treatments, the ratio of P/U isoforms of Cx43 was found to be 89% higher in BM + 1.8mM Fe<sup>+2</sup> treated cells, but was significant at a slightly lower confidence level of 90%.

**Figure 13: An analysis of the effect of various breast milk treatments on phosphorylation of Cx43**



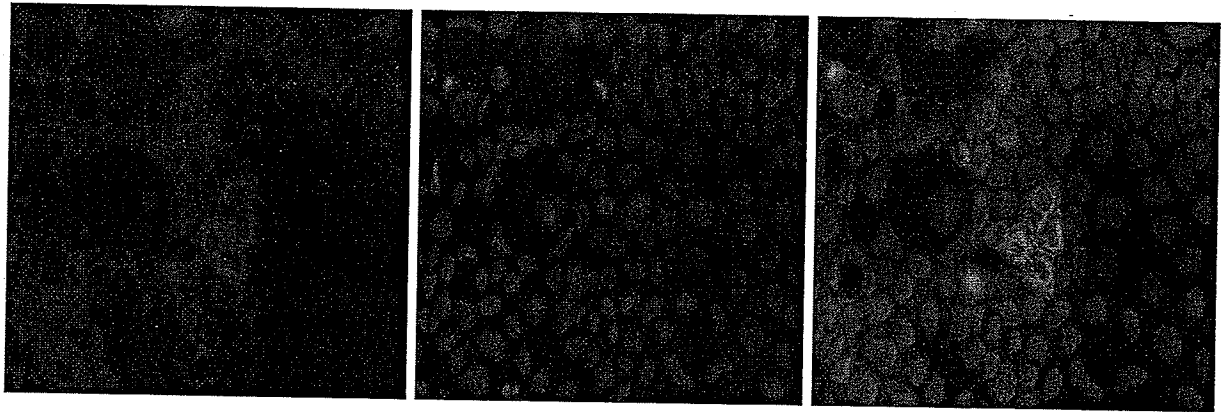
Data shown as mean +/- SEM (N=3). ☆ symbol signifies statistically-significant differences compared to untreated control ( $p < 0.05$ ). △ symbol signifies statistically-significant differences compared to BM only treatment ( $p < 0.10$ ).

### 3.3 Immunolocalization of Cx43:

To observe the localization of Cx43 in untreated CaCo-2BBE cells an immunolocalization experiment was performed (53, 54). Briefly, CaCo-2BBE cells were grown to confluency on 35-mm glass cover slips pre-coated with 2.5% Matrigel®. Cells were then fixed and permeabilized with ice-cold methanol:acetone (50:50) for 1 minute. After blocking with 1% BSA in PBS, cells were incubated overnight at 4°C in primary antibody against Cx43, followed by a 1 hour incubation at 37°C. Coverslips were then carefully washed before addition of secondary antibody (Goat anti-rabbit-alexsa-568) after which they were incubated for 1 hour at 37 °C, then washed and mounted in TBS/glycerol (50:50).

As shown in Figure 14, images 1, 2 and 3 all reveal the punctuate localization pattern typical of Cx43. In panel 1, a nuclear Hoescht stain (1 µg/ml) was added to allow for visible distinction between cell membranes (1A) and cell nuclei (1B). Image 1C is a superimposed view of the first two frames that clearly shows Cx43 localizing in a punctuate pattern along the periphery or cell membrane of CaCo-2BBE cells. Image 4 is a negative control in which the secondary antibody was omitted. Interestingly, there are visible differences in Cx43 signal strength within each image taken indicating that there are variations in Cx43 protein expression and localization among a population of cells.

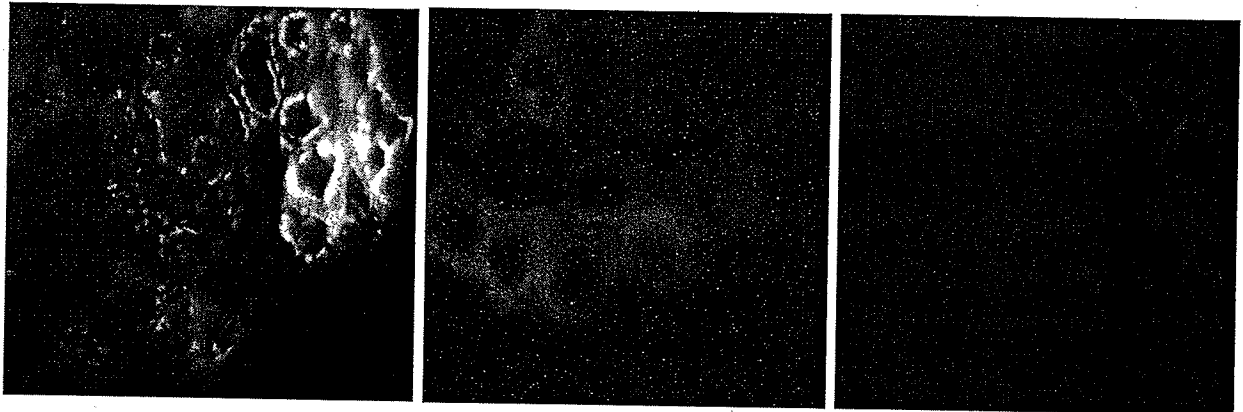
**Figure 14: Immunolocalization of Cx43**



**1A**

**1B**

**1C**



**2**

**3**

**4**

### 3.4 Iron and peroxide decrease gap junctional intercellular communication (GJIC):

To measure GJIC between cells, a commonly used dye scrapeloading technique was employed (55, 56). Briefly, Caco-2BBE cells were grown to confluency (approximately 5-7 days) on glass coverslips pre-coated with 2.5% Matrigel® and cultured in 35-mm Petri plates. Medium was then aspirated from the Petri plate, and coverslips immersed in 1.5 mls of the following treatments: culture medium (control), breast milk (BM), BM + 100  $\mu\text{M}$   $\text{H}_2\text{O}_2$ , BM +  $\text{H}_2\text{O}_2$  + 350 units/ml Superoxide Dismutase (SOD), BM +  $\text{H}_2\text{O}_2$  + 150 units/ml Catalase (Cat), BM + 0.3 mM iron  $\text{Fe}^{+2}$ , BM + 0.9 mM  $\text{Fe}^{+2}$ , BM + 1.8 mM  $\text{Fe}^{+2}$ , BM + 1.8 mM  $\text{Fe}^{+2}$  + SOD, BM + 1.8 mM  $\text{Fe}^{+2}$  + Cat. After a 1.5 hour incubation period at 37 °C and 80% relative humidity, treatments were removed and cells were washed with fresh culture medium. Cells were then incubated in a 0.1% Lucifer yellow/1% rhodamine red admixture in PBS (pH 7.4) for 10 minutes, and this was followed by a wash in 2 mls of PBS. Cells were then fixed with 4% paraformaldehyde (pH 7.2) in PBS.

Due to its small size (MW 450), lucifer yellow enters damaged cells and can rapidly permeate from cell-to-cell through gap junctions (57). Cell coupling via gap junctions was assessed using a fluorescence microscope (Zeiss Axioskop microscope with epifluorescence optics, Sony Power HAD 3CCD colour video camera) by counting the number of contiguous cells labelled with the dye (Figure 15). Rhodamine red was added to each treatment as a control, as it enters damaged cells but is unable to permeate to neighbouring cells through gap junctions because of its much larger size (MW 10,000). Glycyrrhetic acid (100  $\mu\text{M}$ ), a chemical decoupler of gap junctions (58, 59), was added

as a negative control and was incubated for 24 hours to induce complete decoupling of gap junctions.

As shown in Figure 16, GJIC was reduced by 77% compared to untreated controls when cells were treated with glycyrrhetic acid. GJIC in breast milk treated cells was reduced by 35%, although this finding was not statistically significant. In the case of BM with peroxide, GJIC was decreased by 54%. This decrease was slightly attenuated when SOD and catalase were added (50% and 27% respectively); with SOD having a much greater impact on restoring GJIC between cells. When compared to untreated controls iron was found to decrease GJIC in a dose-dependant manner, with low iron concentrations (0.3 mM) reducing GJIC by 38% and high iron concentrations (1.8 mM) reducing coupling by 73%. Again, when both SOD and catalase were added in conjunction with high iron concentrations, GJIC was nearly fully restored to levels found in the control, i.e. coupling was only marginally lower in these samples when compared to the untreated control.

After comparing the BM and the BM + 1.8mM Fe<sup>+2</sup> treatments, GJIC was found to be significantly reduced in BM + 1.8mM Fe<sup>+2</sup> treated cells by 59%, but at an adjusted confidence level of 90%.

Figure 15: Scrapeloading assay

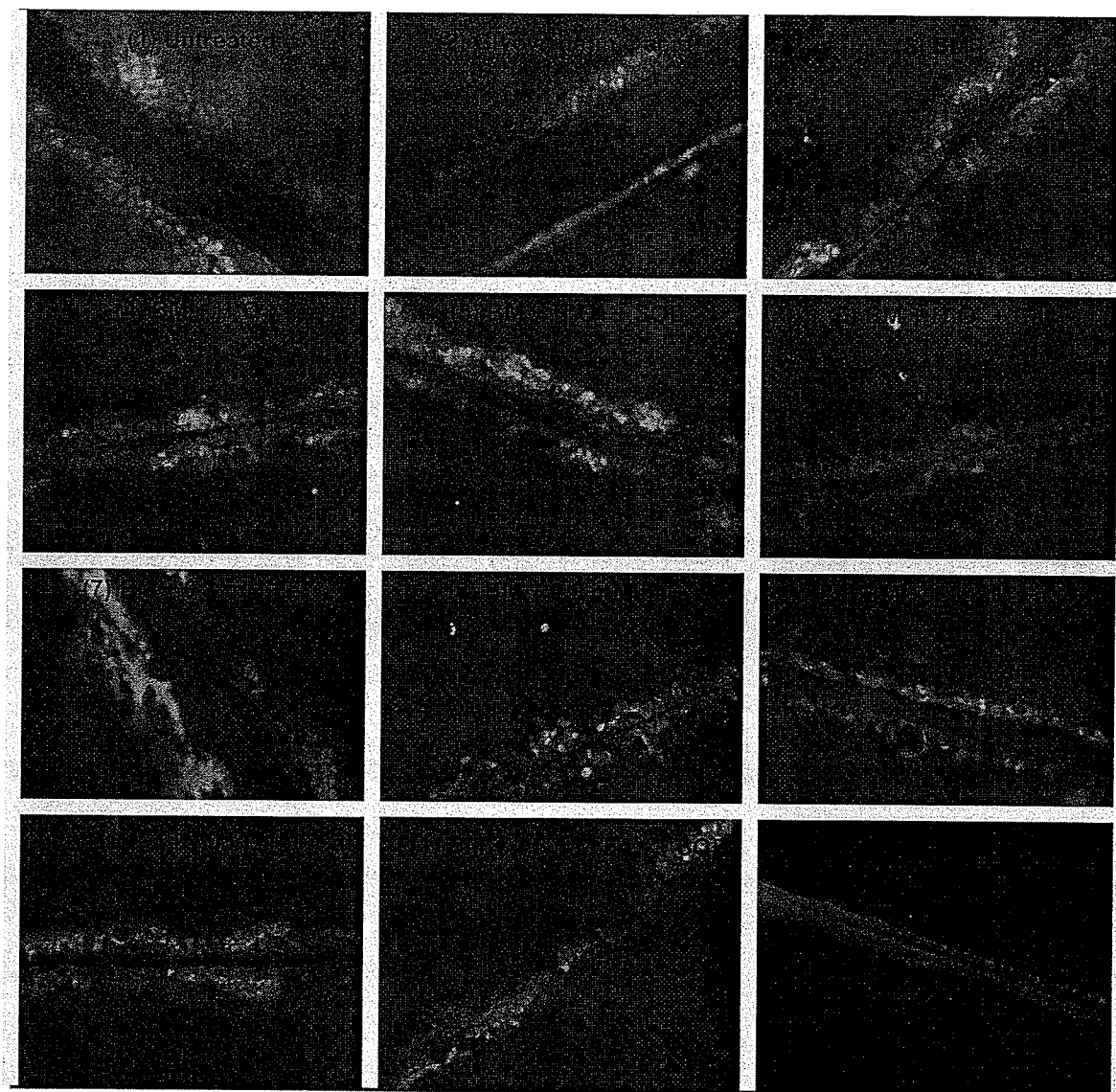
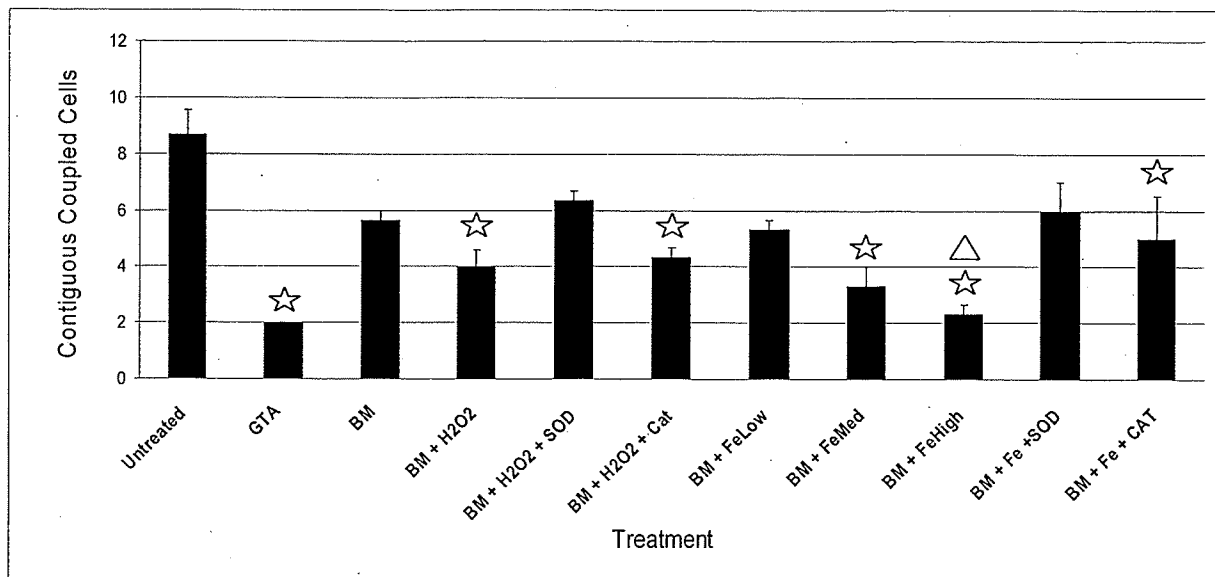


**Figure 16: Effects of various breast milk treatments on gap junctional intercellular communication**



Data shown as mean  $\pm$  SEM (N=3). ☆ symbol signifies statistically-significant differences compared to untreated control ( $p < 0.05$ ). △ symbol signifies statistically-significant differences compared to BM only treatment ( $p < 0.10$ ).

### **3.5 Iron and peroxide decrease transepithelial electrical resistance (TEER):**

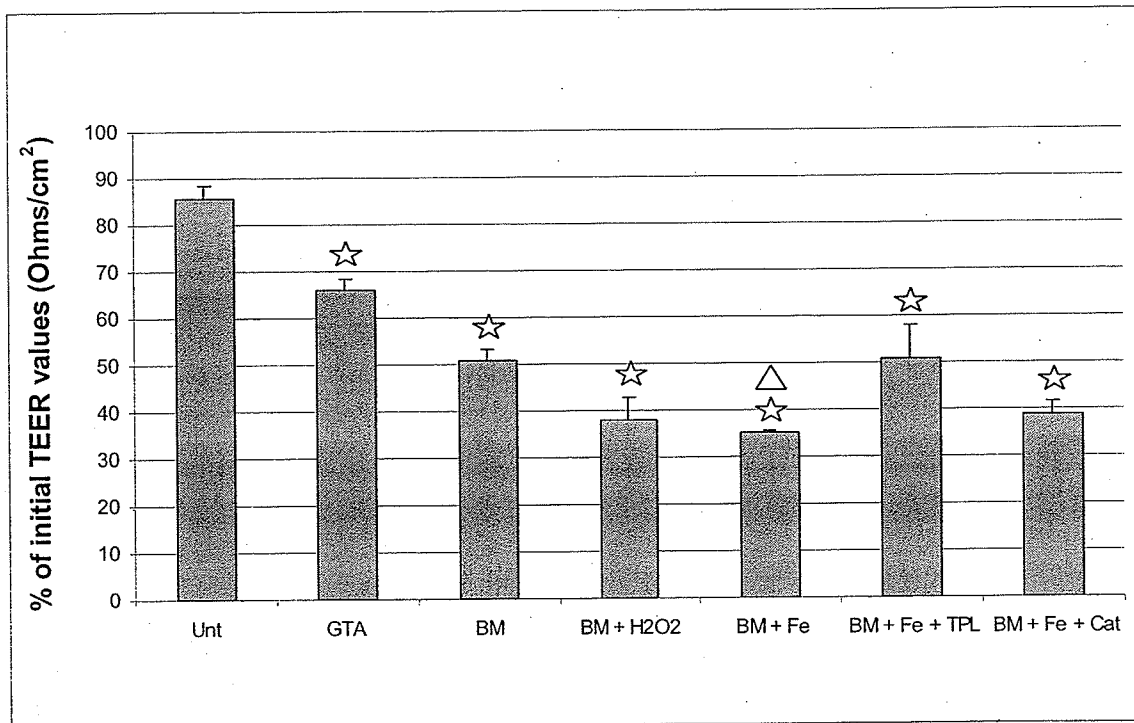
To measure the permeability across a confluent monolayer of cells, the commonly used transepithelial electrical resistance (TEER) assay was employed (6, 60). Briefly, CaCo-2BBE cells were plated onto polycarbonate membranes with 0.4  $\mu\text{m}$  pore size in 4mm diameter transwell chambers at an approximate cell density of  $5 \times 10^5$  cells/well. When cells reached confluency (approximately 14-21 days) measurements of transepithelial electrical resistance (TEER) were made using the WPI REMS Autosampler. When TEER measurements between 500-600 Ohms were taken, which is indicative of a confluent monolayer, 50  $\mu\text{l}$  of the following treatments were added to the apical compartment of each transwell chamber: culture medium (control), breast milk (BM), BM + 100  $\mu\text{M}$   $\text{H}_2\text{O}_2$ , BM + 1.8 mM  $\text{Fe}^{+2}$ , BM + 1.8 mM  $\text{Fe}^{+2}$  + 10 mM Tempol, BM + 1.8 mM  $\text{Fe}^{+2}$  + 150 units/ml Catalase (Cat). Each treatment was incubated for 4 hours at 37°C and 80% relative humidity. Control wells using 100  $\mu\text{M}$  Glycyrrhetic acid were incubated for 24 hours to induce complete decoupling of gap junctions (58,59). Treatments were then aspirated, washed three times with fresh culture medium and final TEER measurements were made.

Final TEER measurements were subtracted from initial TEER readings and the percent difference was expressed. As depicted in Figure 17, TEER was reduced by 23% in GTA-treated cells when compared to untreated control cells. Interestingly, BM-treated cells showed a further reduction in TEER by 40% when compared to the control. When peroxide was added, TEER values were drastically reduced by 56%. A similar trend was observed in BM + iron-treated cells whose TEER values decreased by 59%.

Interestingly, when Tempol and catalase were added in conjunction with BM + iron a slight rescuing effect was observed. Although TEER values were still significantly lower when compared to control cells, they did increase relative to BM + iron treated-cells, with Tempol having a greater impact (41% decrease) and catalase only marginally restoring TEER values (55% decrease).

After comparing the BM and the BM + 1.8mM Fe<sup>+2</sup> treatments, TEER values were found to be significantly lower in BM + 1.8 mM Fe<sup>+2</sup> treated cells by 31%, but only at a slightly lower confidence level of 90%.

**Figure 17: Effects of various breast milk treatments on transepithelial electrical resistance across a confluent monolayer of cells**



Data shown as mean +/- SEM (N=4). ☆ symbol signifies statistically-significant differences compared to untreated control (p < 0.05). △ symbol signifies statistically-significant differences compared to BM only treatment (p < 0.10).

## ***Chapter 4: Discussion***

### **4.1 General outline of this study:**

Oxidative stress is a problem of particular relevance to the pre-term infant, in whom free radical damage is believed to contribute significantly to disorders associated with premature birth (1). Infants born prematurely are at increased risk of intestinal inflammatory disorders, including Necrotizing enterocolitis (NEC). In general, oxidative stress can be considered to be an imbalance between oxidizing and reducing conditions; the former is known to include hyperoxia at the time of birth, while the latter may be considered to be associated with immature anti-oxidant defense mechanisms (1). Recent studies have shown that among the different sources of oxidative stress, dietary supplements commonly added to human breast milk, such as iron, have been shown to generate free radicals (6,7).

One potential target of reactive oxygen species is the gap junction. This complex of channel-forming proteins metabolically and electrically couples neighbouring cells (42). Connexins are the protein subunits that comprise gap junctions, of which there are 21 different forms in the human genome (8,41). Connexin-43 (Cx43) is one of the most widely expressed and well-characterized of these proteins, and there is conclusive evidence that it exists in several different phospho-isoforms.

To investigate the effects of oxidative stress on Cx43 expression and phosphorylation, a human intestinal cell line was used. The physiological endpoints of gap junctions was also explored; namely by looking at how oxidative stress on the enterocyte effects gap junctional intercellular communication (GJIC). An important

function of the intestinal epithelium is to provide a selectively permeable barrier. We therefore also investigated how GJIC may be linked to barrier function.

#### **4.2 Oxidative stress modulates both Cx43 transcript levels as well as protein expression and phosphorylation:**

Caco-2BBE cells were grown in culture and various breast milk treatments known to induce oxidative stress were added. To examine the effects of oxidative stress on Cx43 gene expression a semi-quantitative RT-PCR approach was employed. Both peroxide and iron were used in conjunction with breast milk as inducers of oxidative stress. In the case of peroxide, the initial semi-quantitative analysis demonstrated no significant change in Cx43 gene expression when compared to untreated controls. Interestingly, when iron was added, a decrease in Cx43 expression was observed which closely followed a dose-response curve with low, medium and high iron concentrations each resulting in further decreasing levels of expression.

To confirm the semi-quantitative analysis, real-time PCR (qPCR) was employed which allows for a much more precise and accurate measurement of Cx43 gene expression. In this case, both peroxide and iron significantly reduced Cx43 expression, with high iron concentrations having a slightly greater effect than peroxide. Again, treatments involving iron followed a dose-response curve. Although both results were statistically significant, low iron concentrations had less of an impact than high iron concentrations. Taken together, the results from the qPCR approach indicate that oxidative stress, as induced by hydrogen peroxide or iron, decrease Cx43 gene expression.

After comparing these results to the semi-quantitative study from above, there were noteworthy discrepancies with the treatments involving hydrogen peroxide; whereby the semi-quantitative analysis revealed no change to Cx43 gene expression, but qPCR data showed a significant decrease in expression. A reasonable explanation for this inconsistency is that the peroxide used in the former study was old and had likely been reduced which diminishes its effectiveness.

There have been several studies that support the above findings, whereby oxidative stress causes a decrease in connexin gene expression. An experiment performed by Gagliano et al. explored the effects of ochratoxin A (OTA) treatment on rat liver (62). OTA is a well-known mycotoxin produced by several species of fungi as a secondary metabolite in a variety of human foodstuffs. OTA has severe toxic effects and mainly targets the liver and kidneys. After feeding male Wistar rats toxic levels of OTA, the authors measured the gene expression of three well-known connexins found in the liver through RT-PCR: Cx26, Cx32 and Cx43. Because OTA treatment does mediate toxicity through oxidative pathways it is interesting to note that the authors reached the same conclusion; namely that treatment with OTA significantly reduced all three forms of connexin gene expression.

Another study performed by Gingalewski et al. examined the effects of ischemia/reperfusion injury on Cx32 expression in the liver of male Sprague-Dawley rats (63). Briefly, blood flow to the liver was temporarily blocked with a surgical clamp (ischemia) for 1 hour in duration. This was followed by a reperfusion period where the clamp was removed to allow blood flow into the ischemic tissue. A consequence of the sudden restoration of blood flow results in the generation of oxygen-derived free radicals.

This coupled with the fact that during ischemia/reperfusion, the body's natural antioxidant enzymes are down-regulated (64) an imbalance between stressors and antioxidants is created which leads to the production of oxidative stress. As a result, through quantitative northern blot analysis, the authors observed a decrease in Cx32 gene expression.

To investigate whether iron and hydrogen peroxide affect Cx43 protein expression and its level of phosphorylation, the western blot technique was used. Initially, the native phosphorylation status of Cx43 had to be elucidated. By treating Caco-2BBE cell lysates with alkaline phosphatase, an enzyme that specifically cleaves all phosphate groups from its substrate, Cx43 protein is dephosphorylated. Running a western blot with the cell lysate from these cells along side the lysate from cells that were treated normally (i.e. phosphatase inhibitors included) would reveal Cx43's natural migration pattern. Cx43 was separated into three distinguishable bands, each correlating to a different isoform of the protein. The lowest band represents the unphosphorylated isoform (P0) while the upper two bands represent the phosphorylated forms (P1 and P2) with the higher of the two having a greater degree of phosphorylation (65).

Before studying the effects of iron and hydrogen peroxide on Cx43 protein expression it was necessary to confirm that the antibody stained a protein of both the expected size and location. Cx43 localization was studied via immunofluorescence using untreated Caco-2BBE's. As demonstrated by the immunolocalization results, Cx43 localized in a typical punctuate pattern along the periphery of cells at the plasma membrane. An interesting finding was that, among a confluent monolayer of cells, there appeared to be differences in localization intensity, whereby Cx43 signal was more

evident in some cell clusters than others. One possible explanation for this observation could be the fact that the Caco-2BBE cell-line was isolated as a clone from the parental Caco-2 cell-line which is comprised of a heterogeneous mixture of both colonocyte-like cells and enterocytes; two structurally and functionally different cells (66). It is therefore reasonable to conclude that there are different sub-populations of cells that are expressing Cx43 to varying degrees. In fact, within some cell types there may subsist a more stable group of connexins (67) which further supports the apparent differences in localization. For example, pulse-chase studies have shown that while most connexins have a half-life of 1.5-5.5 hours (68) Cx56 in lens cultures was found to have a subpopulation that had a half-life of over 36 hours (69).

When Caco-2BBE cells were treated with BM and peroxide, total Cx43 expression increased significantly relative to untreated controls. When high iron concentrations were added to cells in conjunction with breast milk, overall Cx43 protein expression was increased even further. A study performed by Azzam et al. yielded a similar finding. In this study they tested the effects of various stressors on Cx43 protein expression using a normal human skin fibroblast cell-line (AG1522)(70). Two such treatments involved the use of ionizing radiation and the chemical t-butyl hydroperoxide, both known inducers of oxidative stress. Through western blot analysis they concluded that these stressors increased Cx43 protein levels indicating that there is may be a link between oxidative stress and increased Cx43 expression.

Another interesting observation from the present study was that, in both of the above cases involving oxidative stress, the level of Cx43 phosphorylation increased significantly while unphosphorylated protein levels, for the most part, remained

consistent with that of the controls. A study undertaken by Bellei et al. supported this finding (71). She and her colleagues used a cell line consisting of normal human keratinocytes (NHK) to study the effects of UVA irradiation (a form of oxidative stress) on Cx43 expression and phosphorylation. Through western blot analysis, they determined that oxidative stress resulted in an increase in the phosphorylated isoform of Cx43.

The results from my study collectively suggest that, when Caco-2BBE cells are exposed to oxidative stress there is a decrease in Cx43 gene expression with a concurrent increase in both total Cx43 protein expression and also the level of its phosphorylation. Treatments involving iron had a slightly greater effect than treatments involving peroxide. It is conceivable that this observation can be attributed to differences in the amount of oxidative stress produced with iron potentially causing a greater degree of stress than peroxide.

#### **4.3 Oxidative stress decreases GJIC and TEER across a confluent monolayer:**

An important function of gap junctions is to allow neighbouring cells to communicate by facilitating passage of various ions, metabolites and second messengers (42). The effect of oxidative stress on gap junctional intercellular communication (GJIC) was explored by using the scrapeloading technique. Glycylthionine acid, a well known chemical decoupler of gap junctions was added to induce complete decoupling of gap junctions in Caco-2BBE cells. When breast milk with peroxide was added to cells a significant reduction in GJIC was observed in relation to untreated controls. Similarly,

when iron was used to stress cells, GJIC was reduced, but to an even greater extent. Again, iron appeared to affect gap junctions in a dose-dependant manner. A similar result was found in a study performed by Hutnik et al. (55). Using a human retinal pigment epithelial cell line (ARPE-19), Hutnik and his colleagues stressed cells by adding the chemical oxidant, *tert*-butyl hydroperoxide and performed the scrapeloading technique. Although the authors found that overall levels of Cx43 were reduced after treatment, a finding which is inconsistent with my data, GJIC did decrease in response to oxidative stress. Hutnik and his colleagues observed a decrease in GJIC as a result of less Cx43 protein expression. My study demonstrated a reduction in GJIC was correlated with an increase in Cx43 protein; which presumably led to non-functional or closed-gated gap junctions. Either scenario is plausible, especially because different cells were tested using different chemical oxidants.

In contrast to gap junctions, tight junctions are the apical-most junctional complexes that connect epithelial cells. They directly contribute to the barrier function of the intestinal mucosa by restricting the passage of solute and water through the paracellular space (72). Interestingly, the tight junction associated protein, ZO-1 has been shown to bind to several members of the connexin family including Cx43 (67). It is therefore reasonable to suggest that GJIC is either directly-linked to epithelial barrier function or indirectly linked through the observation that it contributes to general tissue homeostasis in the gut. In order to test this hypothesis the transepithelial electrical resistance (TEER) across a confluent monolayer of cells was measured before and after exposure to treatment. Although cells treated with glycyrrhetic acid did reveal significantly lower TEER values than control cells, when cells were treated with breast

milk alone an additional decrease in resistance was noted. When peroxide and iron were added in conjunction with breast milk there was an even further decrease.

From the results summarized above, it is reasonable to suggest that there may be links between a decrease in GJIC and barrier function. This finding was supported by a study performed by Iwata et al. (20). Using male Sprague-Dawley rats, these investigators tested the hypothesis that GJIC protects the rat gastric mucosa against ischemia-reperfusion stress. In these experiments, irsogladine and octanol were used, which are a chemical activator and an inhibitor of GJIC respectively. Mucosal damage was assessed in rats by measuring <sup>51</sup>Cr-EDTA clearance across the gastric mucosa. Their results indicate that by inhibiting GJIC, the barrier function in IR stressed rats was impaired.

In the current study, however, treatments which are known to elicit oxidative stress resulted in an even greater reduction in TEER values than did glyceric acid treatment. This indicates that, although a correlation between decreases in GJIC and reductions in TEER were noted, there is clearly additional factors involved. It is reasonable to conclude that oxidative stress may also affect the proteins that comprise of tight junctions in addition to Cx43 which would help explain the further decrease in barrier function.

#### **4.4 Effect of antioxidant additives on Cx43 gene/protein expression as well as on functional properties of gap junctions:**

When Caco-2BBE cells were oxidatively-stressed with either hydrogen peroxide or iron, Cx43 mRNA levels decreased according to the qPCR data. Interestingly, from

the western blot data, overall Cx43 levels increased relative to untreated controls as did the phosphorylated isoform of the protein. According to the data obtained from scrapeloading experiments, GJIC was significantly decreased in response to oxidative stress, and this correlated with a decrease in TEER. The effects of several well-characterized anti-oxidants were examined in each of the above studies. SOD, Tempol and Catalase, all of which are potent free radical scavengers (25), were added in conjunction with either hydrogen peroxide or iron and the restorative effects on Cx43 gene and protein expression as well as on GJIC and TEER, were closely examined. It was concluded that, with one exception, all of the antioxidant enzymes did very little to attenuate the effects of oxidative stress. There were only marginal differences in most cases that could not be deemed statistically significant. With respect to the scrapeloading assay, it is interesting to note that when SOD was added in conjunction with BM and iron, GJIC was restored to levels that were comparable to untreated controls and this finding was statistically significant.

There are several possible explanations as to why the antioxidants did not mitigate oxidative stress in the above studies. As mentioned previously, SOD is a free-radical scavenger that catalyzes the disproportionation reaction of superoxide radicals to produce a molecule of oxygen and hydrogen peroxide:  $O_2^- + O_2^- + 2H^+ \rightarrow H_2O_2 + O_2$  (28).

Tempol is a nitroxide compound that mimics the action of SOD, and is freely cell permeable (73). Catalase on the other hand, metabolizes  $H_2O_2$  into  $H_2O$  and  $O_2$ :



Based on the mechanisms identified above, it is perhaps not surprising that neither SOD nor Tempol had significant effects on peroxide-induced stress. The reason catalase

may not have ameliorated the effects of peroxide treatment may be that the level of intracellular oxidative stress was not high enough to require such action. A more plausible explanation is that cells are not freely permeable to exogenously-added catalase (74), in which case there may be an issue with bioavailability.

In the case of iron-induced stress, a closer look at the mechanism involved will help explain why none of the free-radical scavengers had a greater restorative effect. As mentioned previously, during oxidative metabolism molecular oxygen is reduced to water. In the process, several destructive reaction intermediates are often formed, including superoxide anion, hydroxyl radicals and hydrogen peroxide; all of which are contribute to the production of oxidative stress (75). When supplemental iron is added to BM it can react with naturally occurring  $H_2O_2$  to produce more hydroxyl free radicals through a mechanism involving Fenton chemistry. Iron can also react with lipid hydroperoxides to produce alkoxy free radical (24). Both contribute to the further production of ROS inside cells. Similar to the above, it is not surprising that SOD/Tempol or catalase had little effect on oxidatively-stressed enterocytes due to their respective target radicals.

As mentioned above, it is interesting to note that the addition of SOD to BM and iron treatment did significantly restore GJIC values to levels comparable with untreated controls. It is unclear why SOD did work in this regard, although it may have had subsidiary, less specific effects of free radical generation. It would be interesting to test other potential free radical scavengers such as from the glutathione peroxidase family to resolve this issue.

#### **4.5 A potential model explaining the effects of oxidative stress on Cx43 gene and protein expression:**

When Caco-2BBE cells were exposed to oxidative stress, Cx43 transcript levels were reduced while Cx43 protein levels were found to increase, a seemingly counter-intuitive result. Recent studies suggest, however, that this trend in my experimental findings is both physiologically plausible and consistent. With respect to the decrease in Cx43 mRNA levels, the mechanism by which this happens remains speculative. The aforementioned study performed by Gingalewski et al. might help to explain the decrease in Cx43 gene expression in response to oxidative stress (63). After exposing rat liver to ischemia/reperfusion injury the authors observed a decrease in Cx32 expression levels. They cited a possible explanation for the down-regulation in Cx32 expression in the ischemic liver as being a consequence of the local production of oxygen free radicals during the period of reperfusion. They attributed this to a post-transcriptional event involving the selective degradation of the Cx32 message. It is quite possible that a similar mechanism may be at work in my study.

To account for the increase in Cx43 protein levels in response to oxidative stress, it is necessary to consider the life cycle of connexins. These proteins have a rapid rate of degradation: the protein half-life is 1.5-5.5 hours (68). The life cycle of connexins follow the classical pathway described for many membrane-bound proteins (i.e. ER-Golgi-vesicular transport to membrane). There are several mechanisms by which gap junctions become internalized and eventually degraded. One is via the formation of annular junctions, where an entire GJ plaque is removed from the membrane of two apposing cells (following a typical endocytic pathway). There is still uncertainty however, whether

the gap junctions are actually degraded via the proteasome, lysosome or a combination of both (67).

In the Van Slyke et al. study (68), it was demonstrated that general cytosolic stressors reduce degradation of internalized gap junctions from the cell surface and enhanced gap junction formation and function. Along with heat shock, they also used sodium arsenite, a well-known generator of oxidative stress. After treating S180 cells (sarcoma murine cell line), the authors demonstrated that Cx43 was internalized normally but was prevented from being degraded. Therefore, there was an accumulation of Cx43 inside the cell which translated into an increase in overall Cx43 levels. The authors suggest that many of these internalized connexin proteins can re-aggregate at the membrane to, again, form functional gap junction plaques. This would presumably enhance GJIC which I did not find, so clearly the mechanism is a little more complex.

In a review article written by Laird (67), he unequivocally concludes that phosphorylation of Cx43 proteins plays key roles in regulating the life cycle and function of Cx43. The affect this phosphorylation has on the functionality of gap junctions, however, is still a matter of conjecture. Laird suggests that phosphorylation of connexins may differ considerably among cell types, stages of cell cycle, whether or not the cell-line is transformed, it' 3-D environment, growth factor milieu and extracellular matrix interactions. Several studies support the notion that phosphorylation induces gap junction internalization and therefore inhibition of GJIC. Also, there is not a strong link between the level of phosphorylation of connexins and whether or not they become targeted for degradation (67). In other words, phosphorylation of Cx43 can potentially cause its internalization, but it may have little to do with its degradation. Taken together with the

above, it is plausible that in my study when Caco-2BBE cells are exposed to oxidative stress, an increase in the phospho-isoform of Cx43 is observed which, in turn, leads to an increase in its internalization, while concurrently preventing the connexin degradation pathway from ensuing. Therefore, oxidative stress could induce an overall increase in Cx43 protein (a large portion of which is intracellular and not membrane bound), and a concurrent decrease GJIC due to the reduction of functional gap junction plaques. The study performed by Hutnik et al. supports this finding (55). They state that the increase in intracellular Cx43 localization in stressed cells is consistent with the notion that oxidative stress induces intracellular aggregation of Cx43. Hutnik et al., however, do go on to say that oxidative stress causes the unphosphorylated form of Cx43 to aggregate into nonfunctional dimers while the more highly phosphorylated forms of Cx43 are left unaffected. In my study, I observed the opposite; namely that it is the highly phosphorylated isoforms of Cx43 that are affected with the unphosphorylated form presumably being left intact. Because the affect of phosphorylation on Cx43 is so variable, I speculate each mechanism is equally plausible.

Another study performed by Lin et al. is consistent with my findings (49). Using  $H_2O_2$ , the authors induced stress on the lens of male and female mice (*Mus musculus*). They demonstrated that when the C1B subdomain of Protein kinase C gamma (the primary enzyme involved in phosphorylation of Cx43 in the lens) is oxidized, it results in the formation of disulfide bonds and activation of the enzyme. The activated PKC $\gamma$  phosphorylates Cx43 on Ser368 and this causes disassembly of gap junction plaques and inhibition of gap junction dye transfer activity. Collectively, it remains possible that both effects of oxidative stress could be taking place at the same time. Specifically, oxidative

stress causes an increase in Cx43 phosphorylation which in turn results in disassembly of gap junctions plaques into connexin monomers. From the above, it appears that the same stress prevents internalized gap junctions from being entirely degraded.

It is widely believed that phosphorylation of gap junctions can also affect their gating properties. It results in either an open or closed configuration and this variation is species and tissue-dependant (76). It therefore remains possible that phosphorylation in Caco-2BBE cells could render gap junctions in a closed state and does not necessarily result in their internalization.

Whatever the scenario, the studies outlined above help to explain the observed decrease in Cx43 gene expression and the concurrent increase in Cx43 protein expression and phosphorylation and how these findings may relate to a decrease in GJIC (Figure 18).

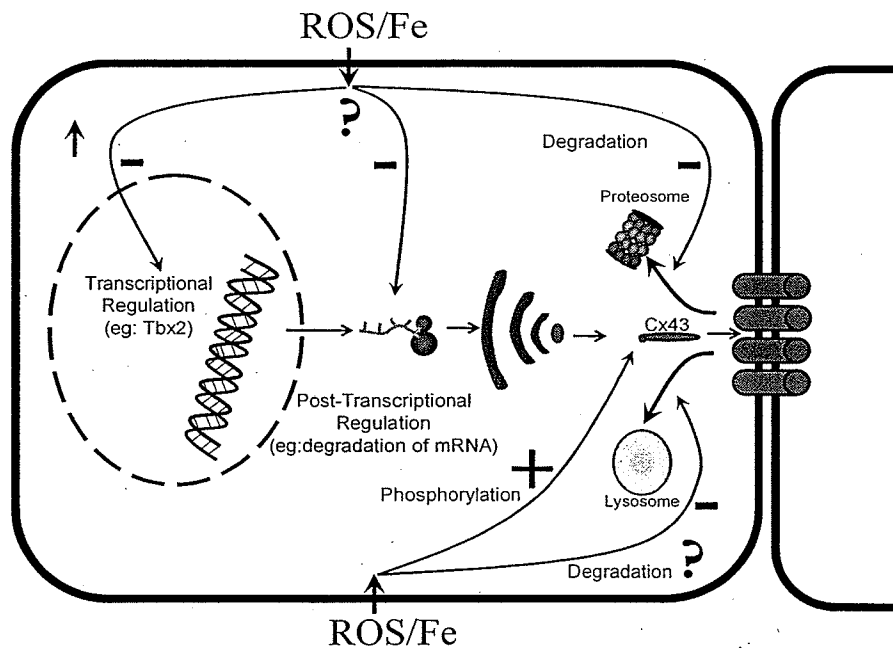


**Figure 18: A model outlining the potential pathways by which oxidative stress affects Cx43 gene and protein expression**

#### **4.6 Oxidative stress and the implications in the human intestine:**

Enterocytes of the human intestine are highly coupled via gap junctions (77) as confirmed through the above immunolocalization experiment. Gap junctions enable individual cells of the intestinal mucosa to communicate with each other allowing the intestine as a whole to act as a functional unit. Through the above studies involving Caco-2BBE cells, I have demonstrated that oxidative stress in the gut decreases Cx43 gene expression while concurrently increasing its protein expression and phosphorylation. From a physiological perspective, as a result of the changes in Cx43 expression, the communication between cells of the intestinal mucosa was altered. Specifically, GJIC in this model of the gut mucosa, was shown to decrease in response to oxidative stress, and this roughly correlated with a decrease in the barrier function as was shown through the TEER data. In the brain, Franteseva et al. demonstrated that oxidative stress is potentiated to neighbouring cells through the opening of gap junctions (increase in GJIC) in a process known as bystander death (10). In myocytes of the heart, Matsushita et al. reported that after inducing hypoxia-reoxygenation decoupling of gap junctions was observed as evidenced by a decrease in GJIC (11). From the former example, it is reasonable to conclude that GJIC was enhanced in the brain in order to try and dissipate the effects of oxidative stress, while in the latter case involving the heart, GJIC was significantly reduced in an attempt to isolate the damage and prevent it from spreading. It is therefore clear that the effect of oxidative stress on gap junctions in the body is highly tissue dependant.

The above alterations in gut physiology can have several potential clinical implications in the preterm infant. A decrease in GJIC was shown to compromise barrier function. In the preterm infant where the gut is already under developed this could translate into an increased risk of bacterial translocation resulting in severe infection, including one of the most dangerous diseases, NEC. Evidence also suggests that GJIC is strongly linked to cell migration (78). As mentioned previously, the cell turnover in the intestine of premature infants is already significantly reduced. Because oxidative stress further impairs this process, it leaves the infants gut in a precarious state. Taken together with the above, I speculate that oxidative stressing the gut could result in such things as an electrolyte imbalance and impaired nutrient uptake in the neonate.

#### **4.7 Summary:**

Pre-term infants often need supplementation in their diet in order to achieve the growth rates they would experience *in utero*. Among the different additives included with a mother's breast milk, iron is important for the developing infant for numerous reasons. Recent studies, as well as the current one, suggest however, that iron can result in oxidative stress in the neonate which, in turn, may translate into severe infection and disease. Among the most prevalent to the premature infant is an intestinal inflammatory disorder known as NEC. The molecular mechanism(s) by which oxidative stress affects intestinal physiology is still relatively unknown. One potential target in the gut are gap junctions, small protein channels that link neighbouring cells together allowing them to communicate via the passage of ions, metabolites and second messengers. Gap junctions are made up of connexin protein aggregates, of which Cx43 is among the most widely

expressed and intensely studied in the human genome. Using a cell model of the human intestine, the effects of oxidative stress on Cx43 gene and protein expression was explored. From a physiological standpoint, gap junctional intercellular communication was also explored, particularly how it relates to barrier integrity. Through the above study, it was concluded that oxidative stress in the human intestine decreases Cx43 gene expression while concurrently increasing overall Cx43 protein levels. These same treatments also increased the level of phosphorylated protein compared to cells that were not exposed to oxidative stress. The communication between cells through gap junctions was also decreased in stressed cells and this loosely correlated to a decrease in barrier function. Several well-known free-radical scavengers were added in conjunction with inducers of oxidative stress, but were found to be relatively ineffective.

## **4.8 Future Directions:**

### *4.8.1 Theoretical perspective:*

The model described above provides a series of plausible pathways by which to explain the observed trends in my experimental findings. While each mechanism discussed has been supported in the literature with other studies, the proposed combined mechanism has yet to be validated. To achieve this, it is important to test each component of the pathway separately. In doing so, this holistic representation of how oxidative stress in the gut affects Cx43 can be substantiated. According to Figure 18, it is possible that gene expression is reduced in response to oxidative stress through a post-transcriptional mechanism involving the degradation of the Cx43 mRNA. To test this hypothesis, one could perform an experiment utilizing various chemical inhibitors of

transcription (e.g. Actinomycin D) and translation (e.g. cyclohexamide). If oxidative stress is causing the selective degradation of Cx43 at the message level, this event would be blocked by the addition of actinomycin D, but not by cyclohexamide (63). It is difficult to rule out that the observed reduction in Cx43 expression may also have occurred at the level of transcription. In fact, a study performed by Chen et al. demonstrated that the transcription regulatory factor, Tbx2 (a member of the T-box gene family) represses expression of Cx43 in osteoblastic-like cells (79). It is therefore reasonable to suggest that oxidative stress may be inducing expression of Tbx2. This would subsequently result in the down-regulation of Cx43 expression. By measuring expression of Tbx2 (or other known regulators of Cx43 expression) by means of PCR, one could determine if this is the likely mechanism.

With respect to Cx43 protein levels, it is plausible that oxidative stress causes phosphorylation of intact Cx43 proteins which subsequently leads to gap junction internalization, but which also prevents the degradative pathway from ensuing. To test this theory, one could incorporate the use of various chemical inhibitors of the degradation pathway. Chloroquine is an effective lysosomal inhibitor and epoxomicin inhibits degradation via the proteosomal pathway. Because it is still unclear which pathway is predominant with regards to Cx43 degradation, by using both chemical means, one could determine whether the increase in Cx43 protein in response to oxidative stress is a result of the prevention of its degradation (68). Another potentially useful tool would be to monitor the localization of Cx43 protein in the gut before and after exposure to oxidative stress. Through immuno-electron microscopy or confocal microscopy the location of Cx43 could be targeted. An increase of intracellular Cx43 would help to

validate the proposed model that Cx43 in the form of gap junctions are internalized but not degraded. Perhaps an even more effective means of verifying this would be to perform a time-course study whereby labelled Cx43 protein could be tracked after cells have been exposed to oxidative stress.

It is also conceivable that phosphorylation of Cx43 in response to oxidative stress affects the gating properties of the gap junctions thereby rendering them in a closed state. To verify if this is a factor in my study, one could transfect live Caco-2BBE cells with an alkaline phosphatase cDNA construct. This would result in the overexpression of phosphatase endogenously which would presumably remove all phosphate groups from native Cx43, predominately resulting in the unphosphorylated isoform. An alternative approach may be to perform site-directed mutagenesis on the known phosphorylation sites of Cx43 preventing the protein from being phosphorylated. A dye transfer study could then be performed as described previously and this would enable one to determine if there is a link between Cx43 phosphorylation and GJIC as a result of the gating properties of gap junctions.

#### *4.8.2 Clinical perspective:*

We have previously shown that iron-supplemented breast milk can cause oxidative stress in the intestine of pre-term infants through the production of oxygen free-radicals. As mentioned above, it is often critical that premature infants be given iron fortification as a means of survival. The question that remains is how do we deal with this? One potential solution would be to investigate different iron-delivery systems to the neonate. Adding iron in the form of ferrous sulphate (as was done in this study) may not be the most effective and safest way. Also, one could look at studying other anti-oxidant

supplements as a means of counteracting the effects of oxidative stress. While the anti-oxidants used in this study had little impact, this still remains a very important consideration when feeding supplemental iron to neonates. By paying close attention to the mechanisms underlying the function of various anti-oxidants it is quite feasible to be able to link certain membrane permeable substances with known antioxidant properties to iron before including it in breast milk.

#### **4.9 Study Limitations:**

The primary objective of this study was to model the effects of iron supplementation on the expression and function of gap junctions in the neonatal intestine. There are several caveats which must be observed, both with respect to the nature of *in vitro* studies, to the specific cells lines used in these experiments, and to the form of iron supplementation.

By their very nature, continuous cell cultures are different from cells encountered in the *in vivo* state: they are in a different cellular milieu, and the genome (and therefore phenotype) of the cells are usually altered. Typically, elements of the genome are lacking, and while cultured cells may mimic the original cells they are intended to model, they may be both morphologically and functionally different.

The cell line used in this study was from an adult human adenocarcinoma intestinal epithelial cell line (Caco-2BBE). My choice of this cell line was predicated on several factors: first, for my purposes, Caco-2BBE cell-line offers a reasonable morphological approximation of both colonic and epithelial cells found in the human intestinal mucosa. They express a brush border similar to both colonic-like cells and

enterocytes, and form confluent monolayers with tight junctions (52). While several of the cell types found in the adult human intestine, including goblet cells, paneth cells and enteroendocrine cells are not expressed in this model, these cells do contain many important adult and fetal markers, such as villin, fimbrin, sucrase-isomaltase, and myosin I and II (52). A second mitigating factor is that the Caco-2BBE line offers the advantages of being very well characterized, and is frequently used in modeling drug delivery and bioavailability studies (7,80). Third, unlike some intestinal cell lines, such as I-407 cultures, these cells are easily maintained *in vitro*.

The Caco-2BBE cells-line does not express mucin, an important mucus layer which would normally exist in the *in vivo* environment. Given that the main goal of this study was to explore the effects of iron-supplemented breast milk on Cx43 gene and protein expression in these cells, it remains to be shown whether the lack of a mucin layer would have made a substantial difference in the bioavailability of iron. Our laboratory has more recently begun characterization a Caco-2BBE/HT-29MTX co-culture model. The latter cell line constitutively expresses mucins, and follow-up experiments may use this particular model.

To my knowledge, there are no human cell-lines derived from the neonatal intestine, aside from FHS 74 Int, a primary culture which does not easily form confluent monolayers and which is morphologically similar to fibroblasts. Therefore, the Caco-2BBE cell line represents a reasonable compromise.

The iron used in this study was in the form of iron sulphate. Stock solutions were first made in water, then immediately added to breast milk at the appropriate concentrations. Although the iron was fully soluble in breast milk, it may have been

interesting to use supplemental iron in the same form that it is fed to pre-term infants. Arguably, there may be some buffering activity in commercial preparations and iron-supplemented formulae. Furthermore, I did not test the stability of iron in breast milk; longer incubation times could conceivably impact on the conversion between ferric and ferrous iron, and possibly increase the level of oxidative stress.

## *Chapter 5: References*

- 1) Robles R, Palomino N, Robles A. Oxidative stress in the neonate. *Early Human Development*, 2001 Nov;65 Suppl: pp S75-81.
- 2) Diplock AT, Charleux J-L, Crozier-Willi G, KOk FJ, Rice-Evans C, Roberfroid M, Stah W, Viiia-Ribes J. Functional food science and defence against reactive oxidative species. *British Journal of Nutrition* (1998) 80, Suppl. 1: pp S77-S112.
- 3) Saugstad OD. Oxygen for Newborns: How Much is Too Much? *Journal of Perinatology*, (2005) 25: pp S45-S49.
- 4) Laborie S, Lavoie JC, Pineault M, Chessex P. Protecting solutions of parenteral nutrition from peroxidation. *Journal of Parenteral and Enteral Nutrition*, 1999 Mar-Apr;23(2): pp 104-8.
- 5) Blackburn ST, Loper DL. *Maternal, Fetal, and Neonatal Physiology*, 1992. Published by W.B. Saunders Company, Philadelphia, PA.
- 6) Diehl-Jones WL, Askin DF, Friel JK. Microlipid-induced oxidative stress in human breastmilk: in vitro effects on intestinal epithelial cells. *Breastfeeding Medicine*, 2007 Dec;2(4): pp 209-18.
- 7) Friel JK, Diehl-Jones WL, Suh M, Tsopmo A, Shirwadkar VP. Impact of iron and vitamin C-containing supplements on preterm human milk: In vitro. *Free Radical Biology & Medicine*, (2007) 42: pp 1591-1598.
- 8) Cruciani V, Mikalsen SO. The vertebrate connexin family. *Cellular and Molecular Life Sciences*, 2006 May;63(10): pp 1125-40.
- 9) Perez Velazquez JL, Kokarovtseva L, Sarbaziha R, Jeyapalan Z, Leshchenko Y. Role of gap junctional coupling in astrocytic networks in the determination of global ischaemia-induced oxidative stress and hippocampal damage. *The European Journal of Neuroscience*, 2006 Jan;23(1): pp 1-10.
- 10) Frantseva MV, Kokarovtseva L, Perez Velazquez JL. Ischemia-induced brain damage depends on specific gap-junctional coupling. *Journal of Cerebral Blood Flow and Metabolism*, 2002 Apr;22(4): pp 453-62.
- 11) Matsushita S, Kurihara H, Watanabe M, Okada T, Sakai T, Amano A. Alterations of phosphorylation state of connexin 43 during hypoxia and reoxygenation are associated with cardiac function. *The Journal of Histochemistry and Cytochemistry*, 2006 Mar;54(3): pp 343-53.
- 12) Seeley RR, Stephens TD, Tate P. *Essentials of Anatomy and Physiology*, 6th Ed, 2007. Published by MCGraw-Hill, New Nork, NY.
- 13) Barker N, van de Wetering M, Clevers H. The intestinal stem cell. *Genes and Development*, 2008 Jul 15;22(14): pp 1856-64.
- 14) Johnson LR. *Essential Medical Physiology*, 2nd Ed, 1998. Published by Lippencott-Raven, Philadelphia, PA.

- 15) Diebel LN, Liberati DM, Dulchavsky SA, Diglio CA, Brown WJ. Enterocyte apoptosis and barrier function are modulated by SIgA after exposure to bacteria and hypoxia/reoxygenation. *Surgery*, 2003 Oct;134(4): pp 574-81.
- 16) Neu J. *Gastroenterology and Nutrition: neonatology questions and controversies*, 2008. Published by Saunders Elsevier, Philadelphia, PA.
- 17) Huber O. Structure and function of desmosomal proteins and their role in development and disease. *Cellular and Molecular Life Sciences*, 2003 60: pp 1872-1890.
- 18) Hollande F, Lee DJ, Choquet A, Roche S, Baldwin GS. Adherens junctions and tight junctions are regulated via different pathways by progastrin in epithelial cells. *Journal of Cell Science*, 2003 116 (7): pp 1187-1197.
- 19) Madara JL, Dharmasathaphorn K. Occluding Junction Structure-Function in a Cultured Epithelial Monolayer Relationships. *The Journal of Cell Biology*, Dec 1985 Volume 101 : pp 2124-2733.
- 20) Iwata F, Joh T, Yokoyama Y, Itoh M. Role of endogenous nitric oxide in ischaemia-reperfusion injury of rat gastric mucosa. *Journal of Gastroenterology and Hepatology*, 1998 Oct;13(10): pp 997-1001.
- 21) Anand RJ, Leaphart CL, Mollen KP, Hackam DJ. The Role of the Intestinal Barrier in the Pathogenesis of Necrotizing Enterocolitis. *Shock*, 2007 Vol. 27, No. 2, pp:124-133.
- 22) Sasaki M, Joh T. Oxidative stress and ischemia-reperfusion injury in gastrointestinal tract and antioxidant, protective agents. *Journal of Clinical Biochemistry and Nutrition*, 2007 Jan;40(1): pp 1-12.
- 23) Winterbourn CC. Reconciling the chemistry and biology of reactive oxygen species. *Nature Chemical Biology*, 2008 May;4(5): pp 278-86.
- 24) Bernotti S, Seidman E, Sinnott D, Brunet S, Dionne S, Delvin E, Levy E. Inflammatory reaction without endogenous antioxidant response in Caco-2 cells exposed to iron/ascorbate-mediated lipid peroxidation. *American Journal of Physiology. Gastrointestinal and Liver Physiology*, 2003 Nov; 285(5): pp G898-906.
- 25) Genestra M. Oxy radicals, redox-sensitive signalling cascades and antioxidants. *Cellular Signalling*, 2007 Sep;19(9): pp 1807-19.
- 26) Rizvi SI, Maurya PK. Alterations in antioxidant enzymes during aging in humans. *Molecular Biotechnology*, 2007 Sep;37(1): pp 58-61.
- 27) Zini R, Berdeaux A, Morin D. The differential effects of superoxide anion, hydrogen peroxide and hydroxyl radical on cardiac mitochondrial oxidative phosphorylation. *Free Radical Research*, October 2007 41(10): pp 1159-1166.
- 28) Afonso V, Champy R, Mitrovic D, Collin P, Lomri A. Reactive oxygen species and superoxide dismutases: role in joint diseases. *Joint, Bone and Spine*, 2007 Jul;74(4): pp 324-9.

- 29) Welty SE. Is There a Role for Antioxidant Therapy in Bronchopulmonary Dysplasia? *Journal of Nutrition*, 2001 131: pp 947S-950S.
- 30) Ran Q, Liang H, Ikeno Y, Qi W, Prolla TA, Roberts II LJ, Wolf N, VanRemmen H, Richardson A. Reduction in glutathione peroxidase 4 increases life span through increased sensitivity to apoptosis. *Journal of Gerontology: Biological Sciences*, 2007 Vol. 62A, No. 9: pp 932-942.
- 31) Flora SJ. Role of free radicals and antioxidants in health and disease. *Cellular and Molecular Biology*, 2007 Apr 15;53(1): pp1-2.
- 32) Rickett, GMW, Kelly FJ. Developmental expression of antioxidant enzymes in guinea pig lung and Liver. *Development*, 1990 108: pp 331-336.
- 33) Dobashi K, Asayama K, Hayashibe H, Munim A, Kawaoi A, Morikawa M, Nakazawa S. Immunohistochemical study of copper-zinc and manganese superoxide dismutases in the lungs of human fetuses and newborn infants: developmental profile and alterations in hyaline membrane disease and bronchopulmonary dysplasia. *Pathological Anatomy and Histopathology*, 1993 423(3): pp 177-84.
- 34) Dani C, Cecchi A, Bertini G. Role of oxidative stress as physiopathologic factor in the preterm infant. *Minerva Pediatrica*, 2004 Aug;56(4): pp 381-94.
- 35) Deng W, Rosenberg PA, Volpe JJ, Jensen FE. Calcium-permeable AMPA/kainate receptors mediate toxicity and preconditioning by oxygen-glucose deprivation in oligodendrocyte precursors. *Proceedings of the National Academy of Sciences of the USA*, 2003 May 27;100(11): pp 6801-6.
- 36) Zhou Y, Wang Q, Mark Evers B, Chung DH. Oxidative stress-induced intestinal epithelial cell apoptosis is mediated by p38 MAPK. *Biochemical and Biophysical Research Communications*, 2006 Dec 1;350(4): pp 860-5.
- 37) Lee JS, Polin RA. Treatment and prevention of necrotizing enterocolitis. *Seminars in Neonatology*, 2003 Dec;8(6): pp 449-59.
- 38) Baylor AE 3rd, Diebel LN, Liberati DM, Dulchavsky SA, Brown WJ, Diglio CA. The synergistic effects of hypoxia/reoxygenation or tissue acidosis and bacteria on intestinal epithelial cell apoptosis. *The Journal of Trauma*, 2003 Aug;55(2): pp 241-8.
- 39) Sanderson IR, Naik S. Dietary regulation of intestinal gene expression. *Annual Review of Nutrition*, 2000 20: pp 311-38.
- 40) Hand GM, Müller DJ, Nicholson BJ, Engel A, Sosinsky GE. Isolation and characterization of gap junctions from tissue culture cells. *Journal of Molecular Biology*, 2002 Jan 25;315(4): pp 587-600.
- 41) Laird DW. Life cycle of connexins in health and disease. *Biochemical Journal*, 2006 Mar 15;394(Pt 3): pp 527-43.

- 42) Warn-Cramer BJ, Cottrell GT, Burt JM, Lau AF. Regulation of connexin-43 gap junctional intercellular communication by mitogen-activated protein kinase. *Journal of Biological Chemistry*, 1998 Apr 10;273(15): pp 9188-96.
- 43) Söhl G, Willecke K. Gap junctions and the connexin protein family. *Cardiovascular Research*, 2004 May 1;62(2): pp 228-32.
- 44) Hachiro T, Kawahara K, Sato R, Yamauchi Y, Matsuyama D. Changes in the fluctuation of the contraction rhythm of spontaneously beating cardiac myocytes in cultures with and without cardiac fibroblasts. *Biosystems*, 2007 Nov-Dec;90(3): pp 707-15.
- 45) Döring B, Shynlova O, Tsui P, Eckardt D, Janssen-Bienhold U, Hofmann F, Feil S, Feil R, Lye SJ, Willecke K. Ablation of connexin43 in uterine smooth muscle cells of the mouse causes delayed parturition. *Journal of Cell Science*, 2006 May 1;119(Pt 9): pp 1715-22.
- 46) Kojima A, Nakahama K, Ohno-Matsui K, Shimada N, Mori K, Iseki S, Sato T, Mochizuki M, Morita I. Connexin 43 contributes to differentiation of retinal pigment epithelial cells via cyclic AMP signaling. *Biochemical and Biophysical Research Communications*, 2008 Feb 8;366(2): pp 532-8.
- 47) Izzo G, d'Istria M, Ferrara D, Serino I, Aniello F, Minucci S. Connexin 43 expression in the testis of the frog *Rana esculenta*. *Zygote*, 2006 Nov;14(4): pp 349-57.
- 48) Rakotovaio A, Tanguy S, Toufektsian MC, Berthonneche C, Ducros V, Tosaki A, de Leiris J, Boucher F. Selenium status as determinant of connexin-43 dephosphorylation in ex vivo ischemic/reperfused rat myocardium. *Journal of Trace Elements in Medicine and Biology*, 2005 19(1): pp 43-7.
- 49) Lin D, Shanks D, Prakash O, Takemoto DJ. Protein kinase C gamma mutations in the C1B domain cause caspase-3-linked apoptosis in lens epithelial cells through gap junctions. *Experimental Eye Research*, 2007 Jul;85(1): pp 113-22.
- 50) Lin JH, Yang J, Liu S, Takano T, Wang X, Gao Q, Willecke K, Nedergaard M. Connexin mediates gap junction-independent resistance to cellular injury. *The Journal of Neuroscience*, 2003 Jan 15;23(2): pp 430-41.
- 51) Kojima T, Murata M, Go M, Spray DC, Sawada N. Connexins induce and maintain tight junctions in epithelial cells. *The Journal of Membrane Biology*, 2007 Jun;217(1-3): pp 13-9.
- 52) Peterson MD, Mooseker MS. Characterization of the enterocyte-like brush border cytoskeleton of the C2BBE clones of the human intestinal cell line, Caco-2. *Journal of Cell Science*, 1992 Jul;102 ( Pt 3): pp 581-600.
- 53) Nemeth L, Maddur S, Puri P. Immunolocalization of the Gap Junction Protein Connexin43 in the Interstitial Cells of Cajal in the Normal and Hirschsprung's Disease Bowel. *Journal of Pediatric Surgery*, 2000 Vol 35, No 6 (June): pp 823-828.
- 54) Qin H, Qing S, Igdoura SA, Alaoui-Jamali MA, Laird DW. Lysosomal and Proteasomal Degradation Play Distinct Roles in the Life Cycle of Cx43 in Gap Junctional Intercellular Communication-deficient and -competent Breast Tumor Cells. *The Journal of Biological Chemistry*, August 8, 2003 Vol. 278, No. 32: pp 30005-30014.

- 55) Hutnik CML, Pocrnich CE, Liu H, Laird DW, Shao Q. The Protective Effect of Functional Connexin43 Channels on a Human Epithelial Cell Line Exposed to Oxidative Stress. *Investigative Ophthalmology & Visual Science*, February 2008 Vol. 49, No. 2: pp 800–806.
- 56) Malone P, Miao X, Parker A, Juarez S, Hernandez MR. Pressure Induces Loss of Gap Junction Communication and Redistribution of Connexin 43 in Astrocytes. *GLIA*, 2007 55: pp 1085–1098.
- 57) Sundset R, Ytrehus K, Zhang Y, Saffitz JE, Yamada KA. Repeated Simulated Ischemia and Protection Against Gap Junctional Uncoupling. *Cell Communication and Adhesion*, 2007 14: pp 239–249.
- 58) Decrouy X, Gasc J-M, Pointis G, Segretain D. Functional Characterization of Cx43 Based Gap Junctions During Spermatogenesis. *Journal of Cellular Physiology*, 2004 200: pp 146–154.
- 59) Davidson JS, Baumgarten IM. Glycyrrhetic Acid Derivatives: A Novel Class of Inhibitors of Gap-Junctional Intercellular Communication. Structure-Activity Relationships. *The Journal of Pharmacology and Experimental Therapeutics*, 1988 Vol. 246, 3: pp 1104-1107.
- 60) Catalioto R-M, Festa C, Triolo A, Altamura M, Maggi CA, Giuliani S. Differential Effect of Ethanol and Hydrogen Peroxide on Barrier Function and Prostaglandin E2 Release in Differentiated Caco-2 Cells: Selective Prevention by Growth Factors. *Journal of Pharmaceutical Sciences*. Published online in Wiley InterScience 2008, May 14: pp 1-13.
- 61) Wang CL, Anderson C, Leone TA, Rich W, Govindaswami B, Finer NN. Resuscitation of Preterm Neonates by Using Room Air or 100% Oxygen. *Pediatrics*, 2008 121: pp 1083-1089.
- 62) Gagliano N, Donne ID, Torri C, Migliori M, Grizzi F, Milzani A, Filippi C, Annoni G, Colombo P, Costa F, Ceva-Grimaldi G, Bertelli AA, Giovannini L, Gioia M. Early cytotoxic effects of ochratoxin A in rat liver: a morphological, biochemical and molecular study. *Toxicology*, 2006 Aug 15;225(2-3): pp 214-24.
- 63) Gingalewski C, De Maio A. Differential decrease in connexin 32 expression in ischemic and nonischemic regions of rat liver during ischemia/reperfusion. *Journal of Cellular Physiology*, 1997 Apr;171(1): pp 20-7.
- 64) Cheng F, Li Y, Feng L, Li S. Effects of tetrandrine on ischemia/reperfusion injury in mouse liver. *Transplantation Proceedings*, 2008 Sep;40(7): pp 2163-6.
- 65) Sato T, Haimovici R, Kao R, Li AF, Roy S. Downregulation of connexin 43 expression by high glucose reduces gap junction activity in microvascular endothelial cells. *Diabetes*, 2002 May;51(5): pp 1565-71.
- 66) Sambuy Y, De Angelis I, Ranaldi G, Scarino ML, Stammati A, Zucco F. The Caco-2 cell line as a model of the intestinal barrier: influence of cell and culture-related factors on Caco-2 cell functional characteristics. *Cell Biology and Toxicology*, 2005 Jan;21(1): pp 1-26.
- 67) Laird DW. Connexin phosphorylation as a regulatory event linked to gap junction internalization and degradation. *Biochimica et Biophysica Acta*, 2005 Jun 10;1711(2): pp 172-82.

- 68) VanSlyke JK, Musil LS. Cytosolic stress reduces degradation of connexin43 internalized from the cell surface and enhances gap junction formation and function. *Molecular Biology of the Cell*, 2005 Nov;16(11): pp 5247-57.
- 69) Berthoud VM, Bassnett S, Beyer EC. Cultured chicken embryo lens cells resemble differentiating fiber cells in vivo and contain two kinetic pools of connexin56. *Experimental Eye Research*, 1999 Apr;68(4): pp 475-84.
- 70) Azzam EI, de Toledo SM, Little JB. Expression of Connexin43 is highly sensitive to ionizing radiation and other environmental stresses. *Cancer Research*, 2003 Nov 1;63(21): pp 7128-35.
- 71) Bellei B, Mastrofrancesco A, Briganti S, Aspite N, Ale-Agha N, Sies H, Picardo M. Ultraviolet A induced modulation of gap junctional intercellular communication by P38 MAPK activation in human keratinocytes. *Experimental Dermatology*, 2008 Feb;17(2): pp 115-24.
- 72) Kojima T, Murata M, Go M, Spray DC, Sawada N. Connexins induce and maintain tight junctions in epithelial cells. *The Journal of Membrane Biology*, 2007 Jun;217(1-3): pp 13-9.
- 73) Chatterjee PK, Cuzzocrea S, Brown PA, Zacharowski K, Stewart KN, Mota-Filipe H, Thiemermann C. Tempol, a membrane-permeable radical scavenger, reduces oxidant stress-mediated renal dysfunction and injury in the rat. *Kidney International*, 2000 Aug;58(2): pp 658-73.
- 74) Klann E. Cell-permeable scavengers of superoxide prevent long-term potentiation in hippocampal area CA1. *Journal of Neurophysiology*, 1998 Jul;80(1): pp 452-7.
- 75) Sinha S, Basant A, Malik A, Singh KP. Iron-induced oxidative stress in a macrophyte: A chemometric approach. *Ecotoxicology and Environmental Safety*, 2008 Aug 13.
- 76) Moreno AP, Lau AF. Gap junction channel gating modulated through protein phosphorylation. *Progress in Biophysics and Molecular Biology*, 2007 May-Jun; 94(1-2): pp 107-19.
- 77) Leaphart CL, Dai S, Gripar SC, Richardson W, Ozolek J, Shi X, Bruns JR, Branca M, Li J, Weisz OA, Sodhi C, Hackam DJ. Interferon-gamma Inhibits Enterocyte migration by Reversibly Displacing Connexin43 from Lipid Rafts. *American Journal of Physiology. Gastrointestinal and Liver Physiology*, July 2008: pp 1-35.
- 78) Pollmann MA, Shao Q, Laird DW, Sandig M. Connexin 43 mediated gap junctional communication enhances breast tumor cell diapedesis in culture. *Breast Cancer Research*, 2005;7(4): pp R522-34.
- 79) Chen JR, Chatterjee B, Meyer R, Yu JC, Borke JL, Isales CM, Kirby ML, Lo CW, Bollag RJ. Tbx2 represses expression of Connexin43 in osteoblastic-like cells. *Calcified Tissue International*, 2004 Jun;74(6): pp 561-73.
- 80) Menconi MJ, Unno N, Smith M, Aguirre DE, Fink MP. Nitric oxide donor-induced hyperpermeability of cultured intestinal epithelial monolayers: role of superoxide radical, hydroxyl radical, and peroxynitrite. *Biochimica et biophysica acta*, 1998 Sep 16;1425(1): pp 189-203.